Since January 2020 Elsevier has created a COVID-19 resource centre with free information in English and Mandarin on the novel coronavirus COVID-19. The COVID-19 resource centre is hosted on Elsevier Connect, the company's public news and information website.

FUNDAMENTALS

CHAPTER 7

ENVIRONMENTAL AND SAFETY ISSUES WITH NANOPARTICLES

CONTRIBUTORS

Hisao Makino (7.1), (7.2.2～7.2.3), (7.3.1)
Hitoshi Emi (7.2.1), (7.4.1～7.4.2)
Akimasa Yamaguchi (7.2.2～7.2.3)
Eiji Iritani (7.2.4), (7.4.3)
Norikazu Namiki (7.2.5), (7.2.6)
Toshihiko Myojo (7.3.2)
Kenji Yamamoto (7.3.3)

CHAPTER 7 ENVIRONMENTAL AND SAFETY ISSUES WITH NANOPARTICLES

7.1 Introduction

Since nanoparticles have superior surface activity and can be applied to the production of particles with various functions, they are extremely important for the future development of sophisticated material technologies. On the other hand, this superior activity of nanoparticles is a cause of trouble from the perspective of safety, and does not always have a positive influence on the environment. Attention must also be paid to impact on health. Nevertheless, all technologies have negative aspects, and overcoming these kinds of problems, we will be able to utilize the superior characteristics of nanoparticles for practical purposes. To achieve this goal, it is necessary to fully understand the influence of nanoparticles on the environment and the relevant safety issues.

This chapter evaluates the relationship between nanoparticles and the environment, and also describes the trouble caused by nanoparticles as well as the safety issues.

The relationship between nanoparticles and the environment will be clarified from the viewpoint of what kind of influence nanoparticles generated either artificially or naturally have on the environment. The influence on the indoor environment, where nanoparticles are produced, will also be clarified.

The safety of nanoparticles will be clearly described from the perspective of the trouble caused by the superior surface activity of nanoparticles; the effect of the compositional characteristics of nanoparticles, and also the influence on health. A method for assessing the influence of nanoparticles using quantum dots is also explained. In the final section, methods for removing nanoparticles from gas and liquid are described as technology to control the influence of nanoparticles on the environment.

7.2 Nanoparticles and environment

7.2.1 Nanoparticles in atmospheric environment

In our atmospheric environment, particles ranging from several nanometers to several tenth micron orders are suspended. They are emitted into the atmosphere at the rate of 2.5 billion tons every year. Emission sources are classified as either natural or artificial.

Natural particles occupy 60% of total particles, consisting mainly of salt particles (~1 billion ton) from the sea and soil particles (~0.5 billion ton) from the land. On the other hand, the latter particles are brought about by human activities. Although occupying only 16% of the total emitted particles, their size is mostly of submicron order and because they contain hazardous chemical components such as nitrates, sulfates, hydrocarbons, heavy metals, etc. in high concentration, their effects on the ecosystem are serious.

Fig. 7.2.1 shows an overview of the size and concentration ranges of various aerosol particles. As it can be seen, the number concentration of atmospheric aerosol which we inhale every day ranges from several thousand particles per cm^3 in clean area to several hundred thousands in dusty areas, and the size range lies between 10 nm and several tens of micrometer.

Fig. 7.2.2 shows mass-based size distribution of atmospheric aerosol particles. Since the size distribution in the nanosize range appears only when the sources of particle generation exist, the size distribution is usually bimodal with peaks in the size range of a few to 10 micron and submicron. The former peak consists of naturally generated coarse particles such as soil dust, sea salt spray, and so on. On the contrary, the latter contains plenty of artificially generated particles, some of which grow from molecules (in most cases vapor state) exhausted by human activities through chemical reaction, condensation, and coagulation. Particle growth rarely leads to particles larger than 1 μm unless high concentration of vapors or particulate matters which cause the above-mentioned growth mechanisms exist in the atmosphere.

As it can be seen from the differences in the particle generation process, fine particles generated from molecules or nanoparticles are much more complicated in their chemical component than the coarse particles, and sometimes have serious adverse health effects. Such fine particles are called PM2.5, which is defined for particles less than 2.5 μm including nanosized particles. Recent epidemiologic investigation reports that the concentration of PM2.5 showed a positive correlation to the mortality due to pulmonary diseases [1].

Various research techniques are used in order to understand the process of particle growth and to trace back to the source of pollution. An example is shown in Fig. 7.2.3 where a characteristic function of sulfur dioxide is shown taking into account all possible factors related to particle growth. Where f is the characteristic function that expresses particle size, particle concentration, particle composition, and so on [2, 3].

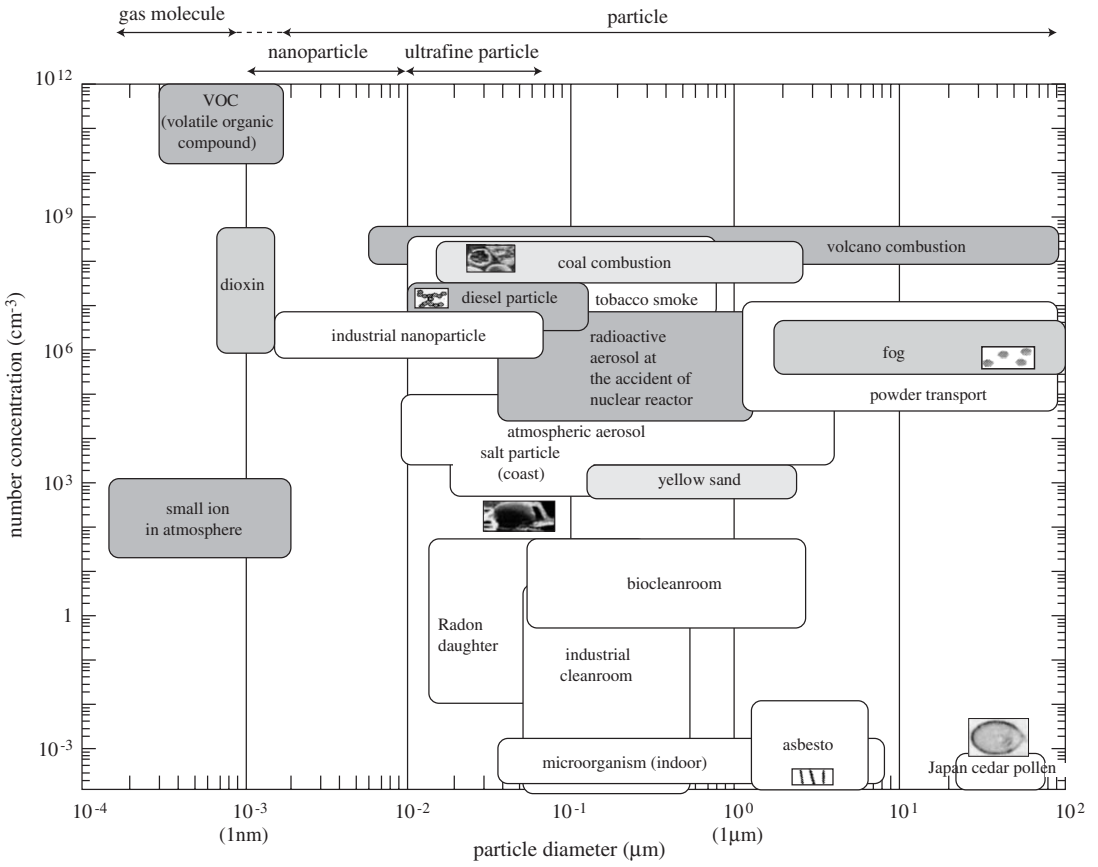

Figure 7.2.1
Particle size and concentration of various aerosols.

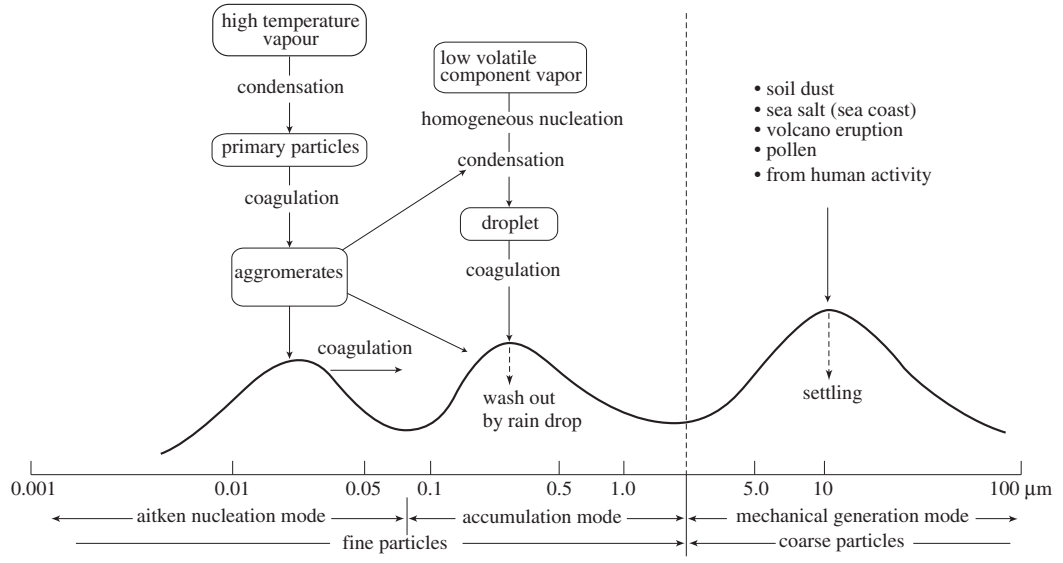

Figure 7.2.2
Mass-based size distribution of atmospheric aerosols.

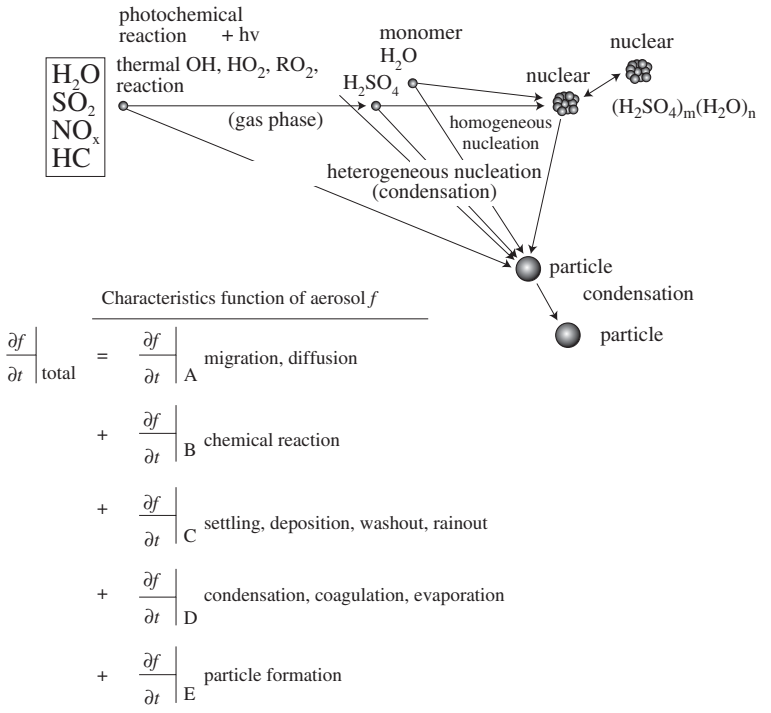

Figure 7.2.3
Generation mechanisms of atmospheric nanoparticles and characteristics function.

References

[1] C.A. Pope, J.M. Thun, M.M. Namboodiri, W.D. Dockery, S.J. Evans, E.F. Speizer and W.C. Heath: *Am. J. Respir. Crit. Care Med.*, **151**, 669–674 (1995).
[2] M. Kasahara: *J. Jpn. Soc. Air Pollut.*, **29**(6), A100 (1994).
[3] M. Kasahara: *J. Jpn. Soc. Air Pollut*., **25**(2), 115 (1990).

7.2.2 Ground water environments and nanoparticles

Particulate materials in water are present in the form of colloids. These colloid particles are classified into inorganic colloids. Examples of the former are oxides of aluminum, silicon and other substances, and typical examples of the latter are substances such as humic acid and fulvic acid. While the structure and molecular weight of particles vary depending on the area of water, it is known that what are usually present in water are comparatively small colloids (particles smaller than 500 nm). The number concentration of colloid particles in ground water, or a typical water area environment, ranges from 10^{11} to 10^{20} (number/m^3) and varies significantly depending on the geochemical conditions of the aquifer.

It is known that in moving water, colloid particles sometimes act as a medium in conjunction with water and in some cases move faster than water.

Fig. 7.2.4 [1] is a conceptual figure showing colloid movement in soil strata. A is a heterogeneous layer composed of macropores formed in rotten roots close to the ground surface. When rain falls, colloids move through macropores saturated with water. B is a saturated

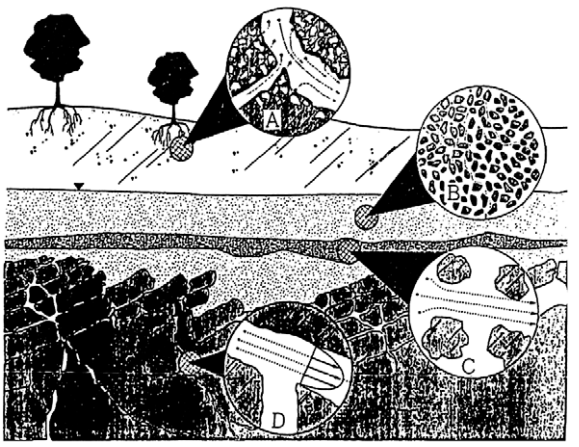

Figure 7.2.4
Concept of colloid movements in soil strata.

homogeneous porous layer such as a sand layer, and most of the colloid particles are trapped. The mechanism of partical trap in this layer is explained by the sand filtration theory. C and D are a gravel layer and a rock bed, respectively, and both have high water permeability with large gaps and cracks. Particles can also pass through easily.

Safety and movement characteristics of colloid particles have a significant influence on the movement of materials such as ionized molecules in aquatic environments. Since fine particles such as nanoparticles in particular are highly stable as colloid particles, it will be very important in the future to understand their influence. At the same time, these characteristics are considered to have a high potential to be developed for further application of nanoparticles.

Reference

[1] S. Nagasaki: *J. Jpn. Soc. Irrigat., Drain. Reclam. Eng.*, **66**(12), 1261–1269 (1998).

7.2.3 Nanoparticles in exhaust gases

In most cases, nanoparticles in exhaust gases are studied from the viewpoint of the influence of total particulate matters on the environment. The term "nanoparticles" is used only in a few cases, "fine particles" is usually used for investigation. Since nanoparticles are part of fine particles, this section will be described from this perspective.

Major sources of combustion exhaust gases are stationary large-scale combustors and diesel engines for stationary and portable use.

For stationary combustors, fuels such as coal, oil, and gas are used. Lighter fuels have a lower rate of particulate emission, but have a higher fine particle content including nanoparticles. Fig. 7.2.5 [1] shows the frequency distribution in combustion of coal and heavy oil. Fig. 7.2.5a and b are the distributions on a number and mass basis, respectively. As these figures clearly show, the total weight of particles of a size of 1 μm or smaller is extremely low, while their total number is, on the contrary, very large. It is clear that,

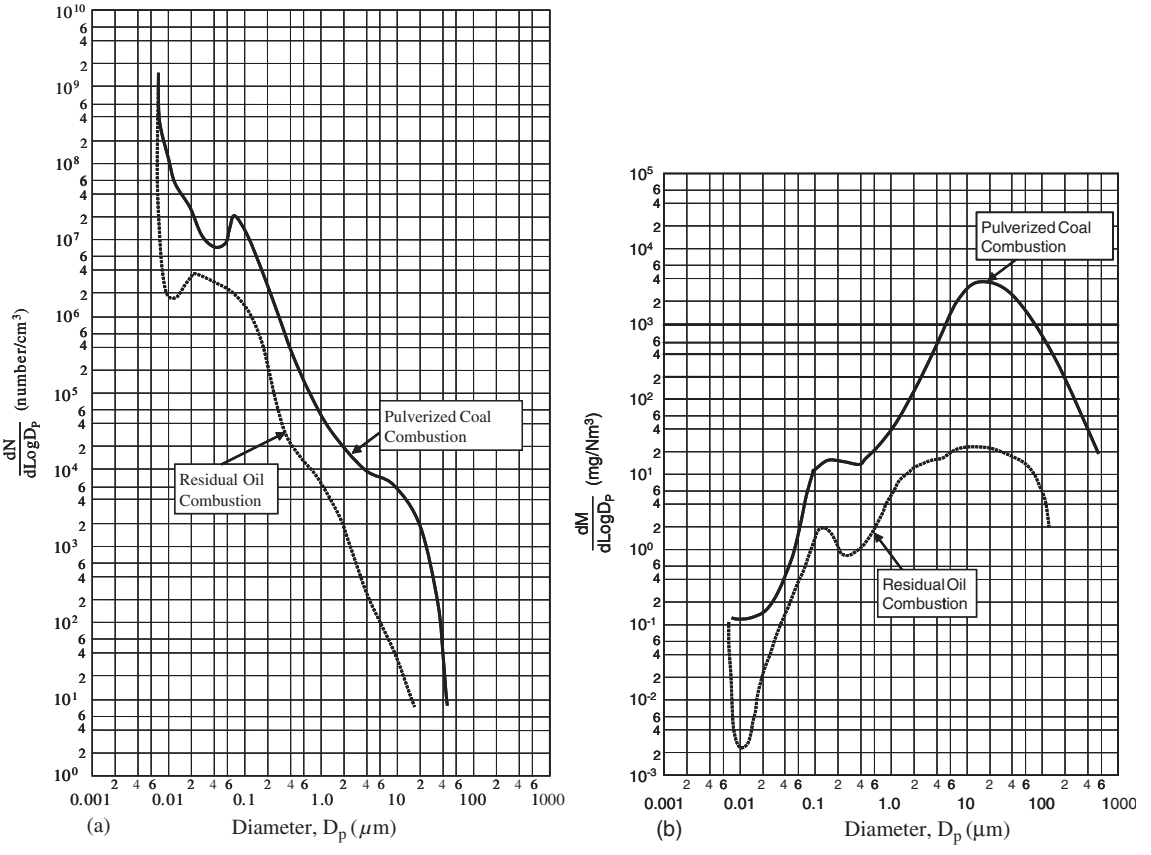

Figure7.2.5
(a) Particle size distribution on number basis at combustor outlet. (b) Particle size distribution on mass basis at combustor outlet.

while the total quantity of particulate material is far larger in coal combustion than in oil combustion, the difference is less when it comes to particles 1 μm or less in diameter, including nanoparticles.

Most of the particles contained in pulverized coal combustion exhaust gases are considered to be formed as particulate materials directly from ash content, which is originally contained in coal and also includes some unburned carbon. Particularly, almost all large-size particles are considered to be this type of particle. On the other hand, fine particles include two types. One type is formed in the process by which low boiling point metal contained in coal ash is evaporated and vaporized in a high-temperature combustion field and then becomes particles in the exhaust gas cooling process. The other includes carbon particles formed in the gas phase, or so-called soot, which is generated due to the delay in oxygen supply for combustion of evaporated volatile matter in the initial stage.

Fig. 7.2.6 [2] shows the relationship between the trace metal content in coal ash and the particle diameter. Aluminum with a high boiling point has a constant concentration regardless of the particle diameter. However it is obvious that in the case of metals with a lower boiling point, the smaller the particle diameter, the larger the content. With regard to particles with sizes 1 μm or smaller in the nano domain, it has been clarified that the generated amount is increased rapidly by reducing combustion air supply or by weakening the oxidation atmosphere in the volatile matter combustion area, for example, when air supply from a burner is reduced in two-stage combustion. This also demonstrates the significant contribution of carbon particles formed in the gas phase.

Also in the case of ash from heavy oil combustion, there are large particles of a carbon residue type generated from sprayed liquid particles and particles formed in the gas phase as well. As in the case of coal, trace metal contained in heavy oil with a low boiling point is concentrated into fine particles and discharged. Also in the case of the combustion of liquefied natural gas, carbon particles formed in the gas phase are generated, albeit in trace amounts.

In contrast, only in the case of diesel engines, fuel is injected into the high-temperature and high-pressure atmosphere produced by compressing only air to induce spontaneous ignition, and combustion continues with a heterogeneous mixture of fuel and air in the combustion chamber. Therefore, particulate materials mainly consisting of unburnt carbon are generated due to incomplete combustion.

Fig. 7.2.7 [3] shows changes in the diameter of particles according to changes in the diesel engine load. It is obvious that the overall concentration of particles increases with the increase in the load rate of the engine. According to observations using SEM, fine particles in diesel engine exhaust gases have also been found to comprise fine primary particles of a size several tens of nanometers, and coarse particles with carbon hydride condensed on the surface of secondary aggregates of primary particles.

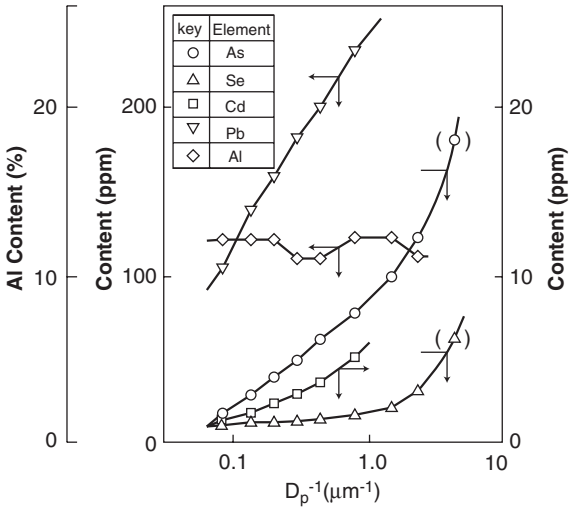

Figure 7.2.6
Influence of particle diameter on trace element contents.

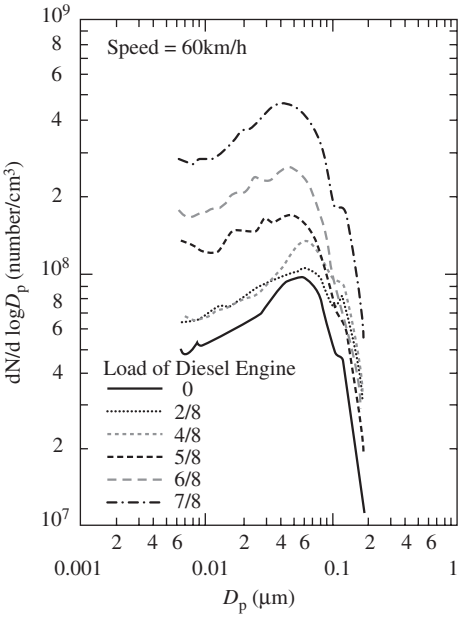

Figure 7.2.7
Particle size distribution measured by DMA.

References

[1] H. Makino: *Denchuukenhoukoku*, 281040 (1982).
[2] H. Makino: *J. Aerosol Res., Jpn.*, **4**(3) (1989).
[3] K. Saito: *J. Soc. Powder Technol., Jpn.*, **38**(7), 493–502 (2001).

7.2.4 Nanoparticles in wastewater

The volume of industrial and domestic wastewater is increasing significantly year by year with the change in the lifestyle based on mass consumption and mass disposal brought about by the dramatic development of the economy and industry. Effective advanced wastewater treatment is required because wastewater contains a variety of constituents such as particles, organic materials, and emulsion depending on the resource.

Inorganic nanoparticles are not generally stabilized in the liquid because they form aggregates of some sort more or less. For wastewater reclamation and reuse, these nanoparticles can be removed from the liquid by the advanced treatment processes such as membrane filtration following biological treatment processes. Organic materials such as macromolecules are regarded as soft nanoparticles judging from their sizes, in contrast with hard inorganic particles.

7.2.4.1 Inorganic wastewater

Chemical mechanical polishing (CMP) is one of the fastest growing processes in semiconductor industry, and it has become an integral part of the state-of-the-art fabrication line for the multilayer wiring board of large-scale integrated circuit (LSI). Besides the semiconductor devices, CMP is widely applied to the magnetic head, the magnetic memory, and the imaging devices. The process is primarily used for polishing the device side of a semiconductor wafer through the mechanical downforce of slurry abrasive in combination with chemical oxidation of wafer surface. In general, colloidal silica is used as abrasive slurry to planarize the oxide wafer surface. Particles in slurry are highly charged to avoid aggregations between particles or between particles and wafer surfaces. During the process, large volumes of ultrapure water are consumed to clean the surface of the wafer, which generates large quantity of CMP wastewater typically having high solid content resulting from slurry abrasive particles of SiO_2, Al_2O_3, or CeO_2, depending on the nature of the CMP application. The quantity of CMP wastewater generated is expected to increase proportionally with the growing needs of the CMP processes. As a result, the treatment and reuse of CMP wastewater has become increasingly necessary. The CMP wastewater has been generally treated with the conventional chemical coagulation–sedimentation process, producing large quantity of sludge. Currently, a membrane filtration process coupled with chemical pretreatment is used to separate the nanoscale particles from the CMP wastewater to reclaim the water [1, 2].

Wastewater of nanosized metal colloid, which is hard to be removed by coagulation–sedimentation process, is discharged in such diverse fields as metalworking factory, electronic components factory, and pigment-manufacturing factory [3]. It is reported that various trace elements of heavy metal are contained in wastewater discharged from a pulp production plant [4]. A spent emulsion, which contains nanosized copper colloid, is discharged from plants manufacturing copper cables for electrical industry, and the treatment for purification of effluents is examined by the integrated membrane system based on ultrafiltration (UF) and nanofiltration (NF) [5]. A glass company generates the wastewater containing fine clay and glass particles from the grinding process of glass surfaces during production of CRT glass used for TVs and monitors. Separation of fine clay and glass particles by microfiltration (MF)/UF is examined in order to treat glass industry wastewater for reuse in the manufacturing process [6].

7.2.4.2 Organic wastewater

The colored substances are free from regulatory constraint of water quality so far because they are not considered hazardous substances. However, water color is being recently used as a standard for the judgment of the purity in water because the removal of color becomes important for wastewater reclamation and reuse.

Dye works are scattered across the country as the industry with local tradition. The dyehouse effluent is discharged in large quantity, and it has extremely complex composition because it contains not only dye but also dyeing aid and finishing agent. In general, dye cannot be removed by standard biological treatment because of its low environmental biodegradability. Dye wastewater is treated by coagulation–sedimentation and activated sludge processes, and nanoparticles produced in the course of the treatment are released into the environment [7].

The color is often imparted by organic substances, predominantly humic substances. Aquatic humic substances including humic and fulvic acids are a term referring to a broad class of naturally occurring mixture of organic compounds, ubiquitous in surface waters, ground waters, and soil pore waters. They are a complex mixture of heterogeneous organic materials in terms of elemental composition, chemical functionality, and molecular size distribution since humic substances can be derived from any organic materials, including plant and animal debris, microfauna, biowaste, pesticide, and others. The molecular weights of humic acids range from several thousands to several tens of thousands daltons, and those of fulvic acids range from several tens of thousands to several hundred thousands daltons. Because of this versatility, humic substances are known to

significantly affect the behavior of some pollutants in natural environments, such as trace metal speciation and toxicity, solubilization and adsorption of hydrophobic organic compounds, and disinfection by-product formation [8].

Melanoidins are natural polymeric compounds of dark brown color, and they are closely related to humic substances. They are produced by a set of consecutive and parallel nonenzymatic reactions taking place between amino compounds and carbohydrates during a Maillard reaction [9]. They are contained in the molasses wastewater from alcohol distillery, sugar processing and refinery industry, and glutamate processing industry. Such wastewater containing melanoidins has frequently caused a coloration problem of water environment, and thus the suitable decolorization treatment is required in many fermentation and sugar industries using molasses. Treatments by flocculation, ozonation, and electrolysis are promising in color removal [10].

Food-processing wastewater usually contains a variety of organic materials in varying degree of concentration. In cheese-making in the dairy products industry, only ~10% of the initial milk volume becomes product, cheese, and the other 90% becomes by-product, liquid cheese whey. Since cheese whey is a protein- and lactose-rich by-product of cheese production, its cost-effective utilization is becoming increasingly important. Recent developments in membrane technology have provided exciting new opportunities for large-scale protein and lactose fractionation in whey treatment [11]. In textile industry, typically it takes over 100 L of water to process just 1 kg of textile material. Not only the washing water must be treated to recover important by-products such as lanolin, but bleaching and dyeing chemicals must also be removed before discharge back to the rivers [12].

Surfactants are a primary constituent of the detergent used in the household routinely, and also they are widely used in industry and agriculture because they have several functions such as washing, emulsification, and dispersion. The surfactants are usually present in the solution in the form of the micelle, and large amounts of surfactant wastewater are discharged in the rivers [13]. Pesticides whose molecular weight ranged from 200 to 400 Da (~1 nm) have been used in great quantities not only for agricultural use but also in golf links and resort. Therefore, the wastewater and effluent treatments have become an important issue, and pesticide separation by NF membranes is found to be very efficient [14].

The potential reclamation of high-quality water produced by the advanced treatment of the secondary effluent of the municipal sewage has come a long way in recent years. The sewage contains various components such as virus [15], pharmaceutical substances [16], and endocrine disrupting compounds derived from zoonotic excretory substances [17]. The advanced treatment of such chemical contaminants at low level becomes increasingly important.

As mentioned above, the removal of nanoparticles contained in wastewater is stringently required to recycle the reclaimed wastewater in a wide variety of industries such as chemical industry, textile industry, pulp and papermaking industry, food-processing industry, dairy products industry, and pharmaceutical industry. Also for domestic wastewater, the reuse of the reclaimed wastewater for nonpotable purposes is becoming more and more important, and this is expected to raise awareness of the behaviors of nanoparticles contained in wastewater in order to upgrade the water treatment processes.

References

[1] J.R. Pan, C. Huang, W. Jiang and C. Chen: *Desalination*, **179**, 31–40 (2005).

[2] H. Umezawa, M. Iseki, D. Takaoka, M. Tsuihiji and T. Kasahara: *Sanyo Tech. Rev.*, **35**(2), 22–30 (2003).

[3] M. Moriya: *J. Jpn. Soc. Water Environ.*, **22**, 346–351 (1999).

[4] L. Skipperud, B. Salbu and E. Hagebø: *Sci. Total Environ.*, **217**, 251–256 (1998).

[5] K. Karakulski, A.W. Morawski: *Desalination*, **149**, 163–167 (2002).

[6] S.K. Kang, K.H. Choo: *J. Membr. Sci.*, **223**, 89–103 (2003).

[7] K. Higashi: *J. Jpn. Soc. Water Environ.*, **20**, 210–214 (1997).

[8] N. Shinozuka: *J. Jpn. Soc. Water Environ.*, **18**, 261–265 (1995).

[9] S. Homma: *Denpun Kagaku*, **38**, 73–79 (1991).

[10] A. Nagano, C. Nakamoto and M. Suzuki: *J. Jpn. Soc. Water Environ.*, **22**, 498–504 (1999).

[11] A. Rektor, G. Vatai: *Desalination*, **162**, 279–286 (2004).

[12] G. Rideal: *Filtr. Sep.*, **42**(7), 30–33 (2005).

[13] K. Yoshimura: *J. Jpn. Soc. Water Environ.*, **16**, 294–301 (1993).

[14] Y. Kiso, H.-D. Li and T. Kitao: *J. Jpn. Soc. Water Environ.*, **19**, 648–656 (1996).

[15] S.S. Madaeni, A.G. Fane and G.S. Grohmann: *J. Membr. Sci.*, **102**, 65–75 (1995).

[16] T. Urase, K. Sato: *J. Jpn. Soc. Water Environ.*, **28**, 657–662 (2005).

[17] S. Kim, Y. Suzuki: *J. Jpn. Soc. Water Environ.*, **25**, 349–354 (2002).

7.2.5 Indoor environments and nanoparticles

In recent urbanized lifestyles people tend to spend more time in enclosed buildings or residences than outdoors. Therefore, it is of great importance to

characterize indoor particles and correlate between indoor and outdoor ones from the viewpoint of evaluating the influence of indoor air quality (IAQ) on human health.

As shown in Table 7.2.1, indoor nanoparticles originate from the several sources such as products of chemical reactions, nonvolatile residues (NVRs) of liquid droplets, printers/photocopiers, combustion, bioaerosols, and infiltration of outdoor air.

Table 7.2.1
Main generation sources of indoor nanoparticles.

Chemical reaction by ozone
Terpenes (α-pinene, limonene) – ozone reaction, formation of irritant products
Nonvolatile residues (NVRs) of droplets
Atomization-type air humidifier and cleaner
Printers
Satellite particles from ink-jet printer, toner-originated matters from laser printer
Combustion
Cooking by gas stoves, cigarette smoking, incense smoking
Bioaerosols
Virus
Outdoor sources
Penetration of outdoor nanoparticles through windows and other house openings

7.2.5.1 Secondary particle formation by gas phase ozonolysis

For particle formation resulting from chemical reaction via ozone, the reaction of terpenes is very common in indoor environments as well as atmospheric ones. Terpenes are emitted from fragrance-containing vegetable oils such as pine oil and citrus oil, and wooden materials including woody furniture [1].

Meanwhile, sources of emission of ozone are air cleaners, air-conditioners, laser printers using corona discharge, and infiltration of outdoor air. Terpenes are generic terms of unsaturated organic compounds that are composed of isoprene as unit (e.g. α-pinene and limonene). These compounds used for household applications readily react with ozone because they have one or more double bonds. It has been proposed that, as shown in Fig. 7.2.8, the reaction mainly proceeds to form less volatile pinonic acid via pinonaldehyde of intermediate [2].

Furthermore, the acid-catalyzed reaction allows the products to convert into higher molecular weight compounds by the polymerization via carbonyl groups in the aldehydes and the aldol condensation [3].

It has been reported that the resultant generated particles have a size distribution with a peak diameter of about 30 nm, and that the products by terpenes ozonolysis irritate human airways [4].

7.2.5.2 Nonvolatile residue (NVR) of liquid droplets

Nanoparticles are also generated from air humidifiers or negative air–ion generators in which water is atomized. In general, humidifiers are mainly categorized into vaporization type and atomization type [5].

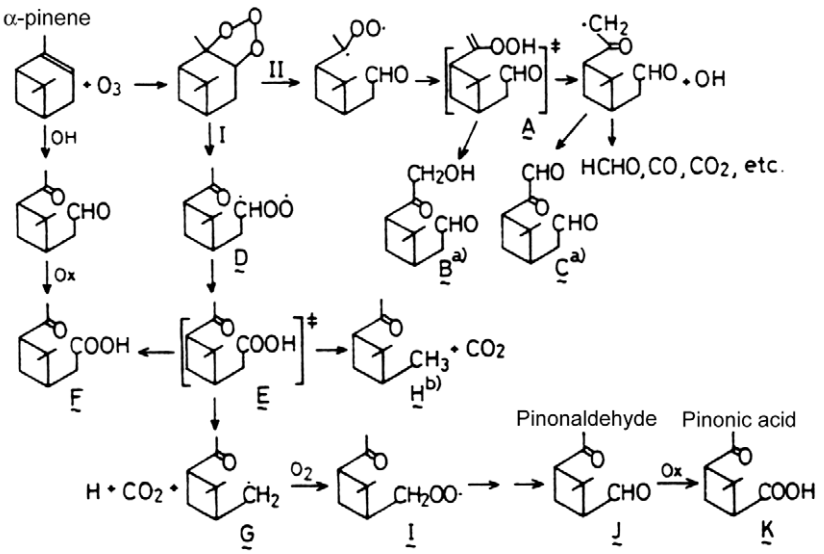

Figure 7.2.8
Reaction path of α-pinene ozonolysis.

The former does not entrain impurities in water when it is fed into indoor spaces of interest. Meanwhile, the latter has the drawback that NVRs are suspended in spaces to be humidified by feeding water via spraying and sonication. The NVRs in tap water include colloidal particles and soluble fraction such as silicates, sulfates, carbonates, and chlorides. The size of NVR particles, D_{p_r} can be estimated from the following equation:

$$D_{p\_r} = D_{p\_m}\sqrt[3]{\frac{C\rho_m}{\rho_r}} \qquad (7.2.1)$$

where D_{p_m} is the droplet size, C the mass fraction of NVR in the droplets, ρ_m the droplet density, and ρ_r the NVR particle density, respectively. Assuming that 2 μm-sized droplets ($\rho_m = 1{,}000$ kg/m^3, $\rho_r = 2{,}500$ kg/m^3) are formed by an ultrasonic nebulizer, and the mass fraction of NVR in city water is 100 ppm (10^{-4}), the NVR particle size, D_{p_r} is estimated to be 68 nm.

Recently, a wide variety of negative ion generators using the Lenard effect, corona discharge, UV/photoelectron emission and electrospray have been commercialized and attention has been focused on features such as air purification and physiological activation [6]. Among them there are the ion generators that atomize water based on the Lenard effect and electrospray form the NVR particles as by-product in addition to ion products if the supplied water contains nonvolatile impurities.

Fig. 7.2.9 shows an example of electrical mobility distribution for ions generated by the electrospray method (positive in this case) [7]. This method atomizes liquid fed to a tip of a capillary electrode to form fine droplets with large amounts of charge by applying high voltage between the tip and the downstream counter electrode. When water in the generated droplets evaporates and their surface charge density attains the charge limit called "Rayleigh limit", this phenomenon induces their self-fragmentation followed by the formation of a high concentration of cluster ions. In this figure, the high-mobility peak on the right side corresponds to the cluster ions. These ions are 2 nm in size assuming that they are singly charged. Meanwhile, another peak on the figure results from NVR in water and then its height increases with the increase in the fraction of tap water in the fed liquid. The electrical-mobility-equivalent size of NVR particles measured by differential mobility analyzer (DMA) – condensation nucleus counter (CNC) method ranges from 10 to 20 nm and their concentration is on the order of 10^4 particles/cm^3. Comparing the forementioned electrical mobility distribution with the particle size one, the NVR nanoparticles are estimated to hold about 100 charges.

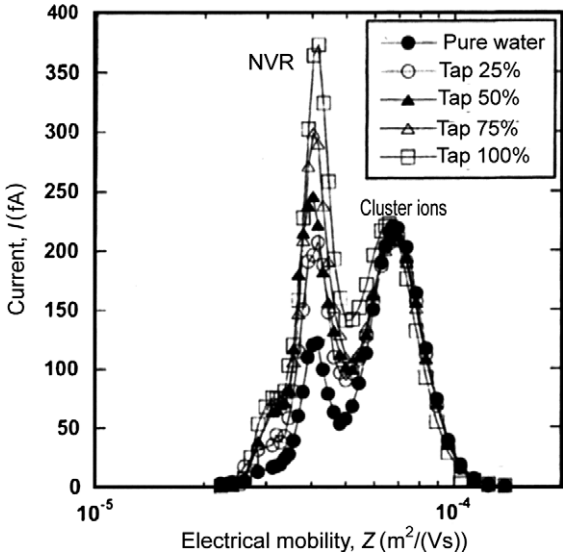

Figure 7.2.9
Electrical mobility distribution of cluster ions and nonvolatile residue (NVR) particles generated by the electrospray method.

7.2.5.3 Laser printers and photocopiers

Accompanying the recent proliferation of computers, the use of inkjet printers and electrophotographic machines such as laser printer and photocopier is becoming common in homes as well as offices. It has been reported that these devices emit various sorts of pollutants. The eco-friendliness-oriented standards such as Blue Angle Standard [8] regulate the maximum permissible limits of benzene, styrene, total volatile organic compounds (TVOC), ozone and particles. As the regulation of particles is based on the emitted mass per hour, mainly the relatively coarser particles such as toner and dust adhering to paper have been targeted. However, some reports have revealed that nanoparticles are emitted from inkjet printers or laser printers [9]. Fig. 7.2.10 depicts the size distribution of particles emitted from a laser printer measured by a scanning mobility particle sizer (SMPS). As seen in the figure, nanoparticles with a peak diameter of around 30 nm are generated in printing mode, whereas the emission in the case of feeding paper without printing is about one third of the normal printing mode. Furthermore, these particles were dried by passing them through a diffusion dryer because they are thought to originate from the nucleation of water vapor emitted from papers in the fixation process. As a result, it was found that most particles formed in the paper feed mode evaporated and then vanished, while particles in the printing mode contained nonvolatile components as well as water. From these results it is anticipated that the particles are derived from styrene remaining in the toner even though their composition has still not been identified.

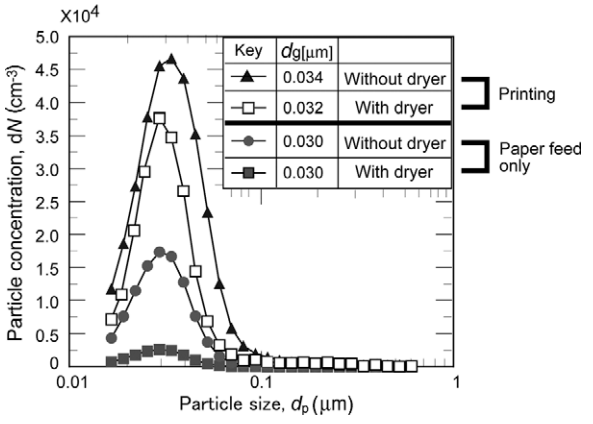

Figure 7.2.10
Size distribution of nanoparticles generated from a laser printer.

Meanwhile, it is thought that during ink discharge ink-jet printers emit not only the main ink droplets but also their satellites (about 1 μm) to result in nanometer-sized NVRs during printing.

7.2.5.4 Combustion

One of the most significant source of indoor nanoparticles relevant to combustion is cooking such as frying and sautéing [10]. Some reports said that over 90% of the particles by number were in the ultrafine fraction range during cooking with bimodal peaks at 60 and 10 nm, attaining the number concentration on the order of 10^5 particles/m^3 and the emission rate of 10^{14} particles/h. Owing to lifestyles in Asian countries, cigarette smoke, incense, and mosquito coils also contribute to indoor nanoparticle levels [11]. It was reported that especially in the Indian subcontinent the combustion of biofuels such as straw and dried cattle manure used for cooking could have a significant impact on climate change in the South Asian region [12].

Sidestream cigarette smoke also contains nanoparticles, having a concentration distribution with the main peak between 0.1 and 0.2 μm [13]. In addition, it was found that nanoparticles a peak size of 30 nm formed by the nucleation of vapor fraction in filtered sidestream smoke immediately after burning when the dilution of smoke by air was insufficient [14]. Attention should be paid to air cleaners when a high concentration of cigarette smoke has to be treated by the cleaners using a single unit air filter.

7.2.5.5 Bioaerosols

Airborne virus particles or virions are typically in the 20–400 nm size range, and are a good example of nanoparticle bioaerosols. Smaller viruses typically contain one subunit, which consists of an outer protein capsid, internal nucleic acid (e.g. DNA and RNA), and other internal proteins. Corona virus that causes SARS and influenza are good examples of them. The viruses most often are transmitted through direct contact with an infected person, such as by shaking hands, hugging or kissing, while sometimes it is spread by nasal droplets. However, it is still unknown how these virus particles behave in the case of airborne infection. Recently, the studies that attempt to elucidate the behavior have been progressing [15].

References

[1] C.J. Weschler, H.C. Shields: *Atmos. Environ.*, **33**, 2301 (1999).
[2] S. Hatakeyama: *J. Aerosol Res., Jpn.*, **6**, 106 (1991) (in Japanese).
[3] Y. Iinuma, O. Böge, T. Gnauk and H. Herrmann: *Aerosol Environ.*, **38**, 761 (2004).
[4] P. Wolkoff, P.A. Clausen, C.K. Wilkins and G.D. Nielsen: *Indoor Air*, **10**, 82 (2000).
[5] T. Ito, K. Nishimura: *J. Soc. Heat. Air-Cond. Sanit. Eng. Jpn.*, **76**, 817 (2002) (in Japanese).
[6] Y. Tanimura: *J. Aerosol Res., Jpn.*, **18**, 20 (2003) (in Japanese).
[7] B. Jan, I.W. Lenggoro, M. Choi and K. Okuyama: *Anal. Sci.*, **19**, 843 (2003).
[8] RAL German Institute for Quality Assurance and Certification: *Basic Criteria for the Award of the Environmental Label* (Printer RAL-UZ 85), p. 35 (2004).
[9] N. Namiki, Y. Otani, H. Emi, N. Kagi and S. Fujii: *Proc. Air Cleaning Contam. Control*, 118 (2003) (in Japanese).
[10] L.A. Wallace, S.J. Emmerich and C. Howard-Reed: *Environ. Sci. Technol.*, **38**, 2304 (2004).
[11] C.-S. Li, F.-T. Jenq and W.-H. Lin: *J. Aerosol Sci.*, **23**, S547 (1992).
[12] C. Venkataraman, G. Habib, A. Eiguren-Fernandez, A.H. Miguel and S.K. Friedlander: *Science*, **307**, 1454 (2005).
[13] K. Katayama, S. Kitao, M. Shimada and K. Okuyama: *J. Aerosol Res., Jpn.*, **19**, 50 (2004) (in Japanese).
[14] Y. Otani, N. Namiki: *Annu. Res. Rep. Smoking Res. Found.*, 795 (2004) (in Japanese).
[15] C J. Hogan Jr., M.-H. Lee and P. Biswas: *Aerosol Sci. Technol.*, **38**, 475 (2004).

7.2.6 Industrial processes and nanoparticles

This section describes the sources of nanoparticle generation in industrial processes by categorizing them into specific processes where a cleanroom is used and other general ones.

7.2.6.1 General industrial processes

The sources of emission of unwanted nanoparticles in general workplaces are categorized as fumes from hot processes (e.g., smelting, refining, and welding) and from (incomplete) combustion processes. Favorable conditions required for the generation of nanoparticles are found in workplaces where there is (1) presence of vaporizable material, (2) sufficiently high temperature to produce enough vapor, followed by condensation to form an independent aerosol, and (3) rapid cooling and a large temperature gradient.

There have been so many studies on occupational exposure to fine particles in the field of public health. In general, high spikes of nanoparticle concentration are observed during active operations, followed by a gradual decay after the operation, primarily because of coagulation, evaporation, dilution, and/or deposition. The fraction of the total number of nanoparticles generally decreases, whereas that of the number of submicrometer particles increases with time and distance from the point of emission. In order to accurately estimate exposure, the effects of spatial and temporal changes will need to be evaluated. Therefore, it is important to identify the time required for the concentration to decline to the normal or background levels.

As an example of reports on grinding processes, Fig. 7.2.11 shows the case where a steel substrate was ground upon using a high-speed grinder [1]. From the figure the distribution of concentration of generated particles has a distinct bimodality, one with the finer peak at around 10 nm and the coarser one at around 1 μm. The former results from within the grinder motor and the volatilization or combustion of amenable ground substrate and/or grinding materials, the latter from the mechanical abrasion and attrition. However, the resultant total concentration on the order of 10^5 particles/cm^3 is not so high.

7.2.6.2 Industrial processes with cleanrooms

Cleanrooms and associated controlled environments (e.g., in the case of an ISO Class 3 cleanroom, the maximum permissible airborne particle concentration is less than 10^3 particles/m^3 for particles with the size of 0.1 μm or larger, while the airborne particle concentration in ordinary indoor environments is on the order of 10^9 particles/m^3 or higher) are usually adopted to avoid particle contamination in industrial processes where precision products such as engineered nanoparticles, semiconductors, and other electronic or optical devices are fabricated because the deposition of particles onto product surfaces causes their yield reduction and quality deterioration. The emission sources in cleanroom environments are tabulated in Table 7.2.2. Since some of the listed emission sources emit trace amounts of nanoparticles, these nanoparticles are not regarded as particulate contaminant but as chemical or molecular one. In this section, these nanometer-sized solid substances formed on solid surfaces by chemical reaction are also included.

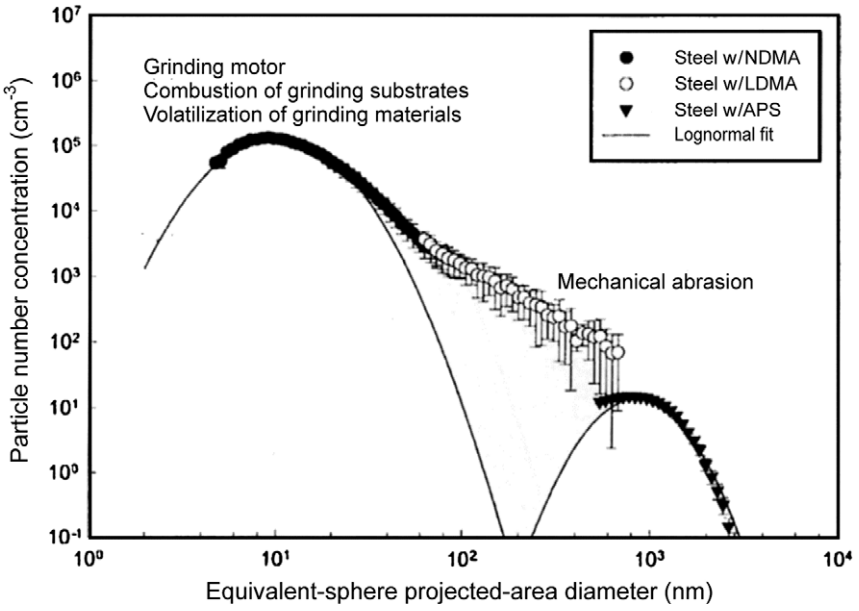

Figure 7.2.11
Size distribution of nanoparticles generated when a steel plate was ground with a high-speed grinder.

Table 7.2.2
Main sources of emission nanoparticles in cleanroom environments.

Exhaled air of human
Corona-discharge ionizer (e.g. gas-to-particle conversion of low-molecular-weight cyclosiloxane)
Boron-containing particles from borosilicate glass fibers of HEPA filter
Haze by chemical reaction on solid surfaces (precipitation of ammonium salt and silica)
Watermark on wafer surfaces at drying
Leakage from thin film and nanoparticles processing equipment

(1) Air exhaled by humans

Emissions from human bodies are a minor contribution in ordinary indoor situations because airborne particle concentration in such places is quite high, whereas the emission cannot be seen as negligible in cleanroom environments. The major human emissions are thought to be atmospheric dust deposited on clothes and skin fragments, and most of these particles are submicrometer in size. Meanwhile, particles in exhaled air are composed of fine liquid droplets from spittle (99.5% of water), and then evaporate to form nanoparticles of NVR.

In Fig. 7.2.12 an example of size distributions of particles in exhaled air before and after smoking is shown [2]. When measuring particles in exhaled air, the air was introduced into a measuring device after drying them by passing them through a diffusion dryer. The size distribution of particles in exhaled air before smoking ($N_{db} = 0$) has a bimodality, one with the peak size of 0.2 μm, and the other of 20 nm or smaller. The former peak comes from atmospheric aerosols as it decreases with the increase in number of deep breaths in a clean booth (N_{db}). The latter originates from NVR particles of spittle droplets.

Incidentally, since smoking induces the rapid increase in number concentration of particles 0.1 μm or larger by 10^4 times or more and for nanoparticles by about double, special attention should be paid to the management of personnel's clothes such as face mask when they enter a cleanroom after smoking.

(2) Emission from ionizers

Ionizers are commonly used in cleanrooms to eliminate electrostatic charge on substrates for precision electronic devices. The most popular ionizer is a corona-discharge type.

Corona-discharge type ionizers are categorized into the following three groups; AC, DC and pulsed-DC types. The issues of emission of contaminants such as ozone, NO_x and particles have been pointed out [3]. These issues are also applicable to air cleaners using a corona discharger. Among these problems is that the particle emission has a potential for particle contamination onto product surfaces and eventually decline in product yield.

The particle emission, which has been studied since the 1990s, is caused by foreign particle deposition onto electrodes, electrode erosion, and gas-to-particle conversion. The issue of electrode erosion can be solved by the improvement of electrode materials, whereas for the issue of gas-to-particle conversion, the airborne molecular contamination (AMC) control to be ionized has to be made. It was reported that

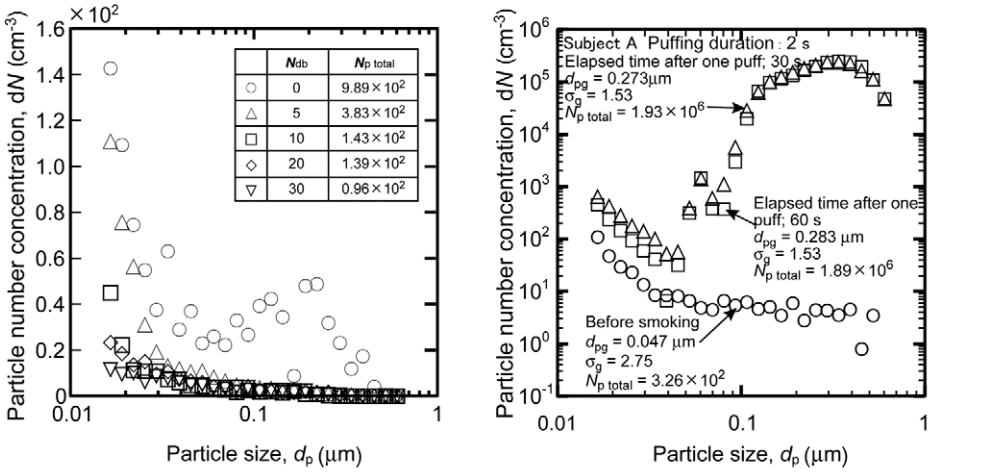

(a) Change in particle size distribution with the number of deep breathings by subject A

(b) Change in particle size distribution with the elapsed time after one puff of smoke by subject A

Figure 7.2.12
Size distribution of particles in exhaled air for smoking subjects.

silicon-containing compounds that precipitated on the electrodes result from the gas-to-particle conversion of low-molecular-weight cyclosiloxane (LMCS) from silicone sealant via corona discharge [4].

(3) Boron-containing particles from HEPA filter with borosilicate glass fibers

The use of HEPA and ULPA filters made of borosilicate glass fibers prevails in the most cleanrooms. It has been known that owing to chemical reaction in equation (7.2.2) BF_3 vapor is formed from glass fiber filters by passing HF gas leaking from wet cleaning equipment through the filters. Boron, which is a dopant element for semiconductors, has been thought to be a contaminant that might cause failure in semiconductor devices if it comes from the surroundings. In addition, it has been revealed that trace amounts of boron in the form of boric acid (H_3BO_4) are also formed from the fibers via the reaction with moisture in the surrounding air (equation (7.2.3)).

Fig. 7.2.13 depicts the change in volatilized boron mass from various filters in terms of airborne boron concentration. Especially, at the initial stage just after the initiation of ventilation, the volatilized boron mass increases with increase in relative humidity [5]. Boric acid, which is solid at room temperature, is surmised to form in the particulate form. However, its existence was identified only by chemical analysis because it is present only in trace amounts.

$$B_2O_3 + 6HF \rightarrow 2BF_3 + 3H_2O \qquad (7.2.2)$$

$$B_2O_3 + 3H_2O \rightarrow 2H_3BO_3 \qquad (7.2.3)$$

(4) Haze on solid surfaces by chemical reaction

Haze might form on glass surfaces of lenses and mirrors for optical instruments if they are exposed for a long time to cleanroom environments where AMCs are not controlled properly. The haze is more likely to bring about the insufficient light delivery onto a surface to be exposed in photolithographic processes. One of the reasons is that ammonium sulfate ($(NH_4)_2SO_4$) is formed, which then precipitates on the glass surfaces via chemical reaction of sulfur dioxide (SO_2) with ammonia or amines.

For another reason, hexamethyldisilazane (HMDS) used as additive in resist coating or LMCS from silicone sealant is adsorbed, and then decomposed to form silica precipitates on glass surfaces by photochemical reaction during laser irradiation, followed by the unwanted decline in laser penetration [6]. As another example a report said that tiny projections, which are also known as "haze", with a size of 0.2 μm or smaller were formed on silicon wafer surfaces owing to the adsorption of organosilicate compounds in thin film formation processes with CVD. It is similarly caused by the precipitation of SiO_2 [7].

(5) Watermarks on solid surfaces during drying

When a silicon wafer surface is cleaned with deionized water and then dried in air, a watermark is formed on it via the mechanisms demonstrated in Fig. 7.2.14. Oxygen in air is dissolved and diffused into water droplets or adsorbed water on a wafer surface, followed by the formation of silicate compounds via silanol reaction. The watermark on a wafer

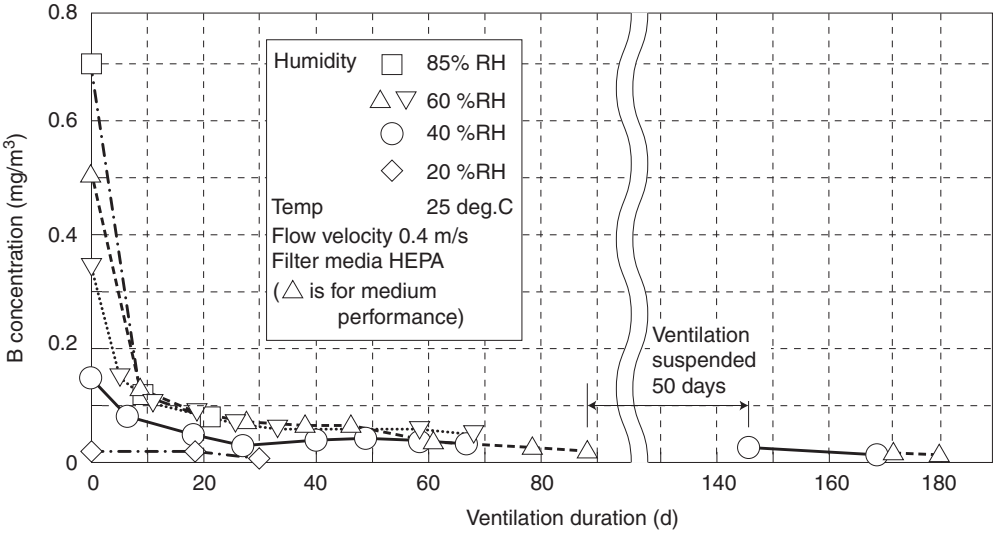

Figure 7.2.13
Change in concentration of boron emitted from various filters at different relative humidities.

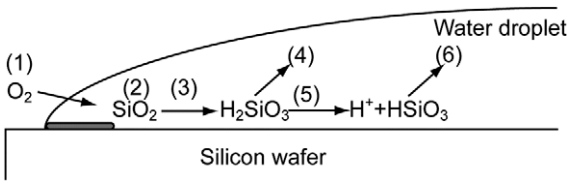

Figure 7.2.14
Mechanism of watermark formation on a silicon wafer surface.

surface is detected in the form of nanometer-sized particles by an electron microscope [8].

(6) Leakage from nanoparticle production processes

In regard to the risks to processing equipments by nanoparticle leakage from production processes, the VDI report in Germany [9] has been described in detail. The production of engineered nanoparticles can be generally categorized into two approaches. One is a "top-down" approach that is initiated with a bulk material and then breaks it into finer pieces using some form of energy such as etching, ball milling, sputtering, and laser ablation. The other approach is to synthesize materials from the atomic or molecular level by growth and assembly to form the desired nanoparticles. Processes included in this "bottom-up" category are sol-gel, chemical vapor deposition, flame synthesis laser pyrolysis, and so on.

Most of these processes are performed in a closed reaction chamber installed in a cleanroom or associated controlled environment. Human exposure to these engineered particles does not take place during synthesis unless there is an unexpected system failure (e.g. rupture of a seal). Human exposure is more likely to occur after the manufacturing when opening the reaction chamber, drying the products, or in the post-process handling of the products.

The release of nanoparticles during production chamber cleaning operations is another critical point. Cleaning typically involves using water or some solvent. Brushes, sponges, or tissues used in the cleaning will carry nanoparticles into the waste stream. Disposal of the waste and wastewater may become a source of nanoparticle release into the environment.

Further, conditioning of nanoparticles such as compression, coating, and composition to form final products may also result in the release to the environment and resultant exposure although very few studies have been carried out on this subject. Recent studies [10] to evaluate the aerosol discharge during the handling of carbon nanotubes showed that the generation of nanoparticles occurred under vacuum to remove spilled nanotube materials or vigorous mechanical agitation. However, they reported that the concentrations were very low. In addition, measurements of nanoparticle levels during final packaging of carbon black, which is a typical engineered nanoparticle material, showed that there was no increase in nearby air [11].

References

[1] A.T. Zimmer, A.D. Maynard: *Ann. Occup. Hyg.*, **46**, 663 (2002).
[2] Y. Otani, N. Namiki: *Annu. Res. Rep. Smoking Res. Found.*, 747 (2005) (in Japanese).
[3] M. Suzuki, Y. Yamaji, *J. Jpn. Air Cleaning Assoc.*, **32**, 218 (1989) (in Japanese).
[4] N. Namiki, Y. Otani, H. Emi and S. Fujii: *J. Inst. Environ. Sci.*, **39**, 26 (1996).
[5] K. Kato, A. Tanaka, A. Saiki and J. Hirata: *Proc. Air Cleaning Contam. Control*, **5** (1995) (in Japanese).
[6] Y. Ushio, T. Nakamura, S. Shimizu, T. Oshino, K. Matsuda and T. Arai: *Proc. Air Cleaning Contam. Control*, 335 (1998) (in Japanese).
[7] A. Saiki, S. Ro and T. Fujimoto: *Chemical Contamination in Semiconductor Processing Environments and its Countermeasures*, Realize, Inc., Tokyo, 426 (1997) (in Japanese).
[8] The Japan Society of Industrial Machinery Manufactures: Report on Behavior Control of Individual Sort of Contaminants – *1993 Report on Introduction of Advanced Technologies to Environmental Equipment Industry*, 171 (1994) (in Japanese).
[9] W. Luther: *Industrial Application of Nanomaterials – Chance and Risks*. Future Technologies, Division of VDI Technologiezentrum, Düsseldorf, Germany, p. 112 (2004).
[10] A.D. Maynard, P.A. Baron, M. Foley, A.A. Shvedova, E.R. Kisin and V. Castranova: *J. Toxicol. Environ. Health A*, **67**, 87 (2004).
[11] T.A.J. Kuhlbusch, S. Neumann and H. Fissan: *J. Occup. Environ. Hyg.*, **1**, 660 (2004).

7.3 Safety of nanoparticles

7.3.1 Problems caused by nanoparticles

Study on the safety of nanoparticles has started only recently, and no sufficiently systemized results have been obtained. What should be noted in particular is that the possibility of radial troubles caused by particulate matters are considered to increase by the decrease of particle diameter in nanoparticles.

One typical example is the problem of dust explosion, caused by the high surface reactivity of fine particles. In other words, since nanoparticles are extremely fine particles, dust explosion is more likely to occur. Explosion is more likely to occur because fine particles are different in their composition, in that low boiling point metal can be easily condensed, as described in Section 7.2.

However, of particular note here is that, since all particles do not necessarily exist independently in the form of a single particle, the possibility of dust explosion does not simply increase as particles become finer.

Fine particles with sizes of 1 μm or smaller such as nanoparticles have an extremely high agglomeration propensity and secondary particles can be easily generated. Therefore, in some cases they conversely behave like large particles. These are the points to be taken into consideration when studying the problems caused by nanoparticles.

As shown in Fig. 7.3.1 [1], the effect of the particle diameter on dust explosion tends to be that the smaller the particle diameter of the dust, the lower the minimum explosion concentration. In other words, explosion can be induced under conditions of lower concentration of particles in air as the particle diameter becomes smaller. Due to the difficulty of conducting experiments to suspend particles with the same size in a uniform concentration, this result was obtained from particles far larger than nanoparticles; however, it has been clarified qualitatively that the smaller the particle diameter, the higher the possibility of dust explosion.

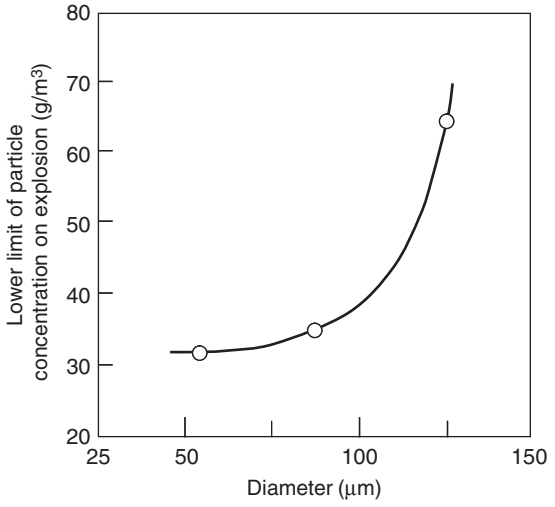

Figure 7.3.1
Influence of particle diameter on lower limit of particle concentration for explosion.

From the perspective of composition, the possibility of explosion increase if materials that react easily with oxygen at low temperature are condensed into particles of small diameter. Therefore, with regard to the effect of particle diameter on dust explosion, more careful attention needs to be paid in the case of combined materials than in the case of uniform materials, as assumed in Fig. 7.3.1. As described before, however, since nanoparticles are considered to exist often as agglomerates, it is necessary from the perspective of the particle diameter to take into consideration the diameter of not only primary particles but also of particles after agglomeration. To address the safety of nanoparticles, it will be important in the future to elucidate their behavior in detail including these factors.

Reference

[1] H. Enomoto: Funjin-Bakuhatsu–Kikensei hyouka to Boushi taisaku (Dust explosion–Estimation of danger and control policy), Ohmsha, Ltd., Tokyo, 17 (1991).

7.3.2 Health effects on nanoparticles

The terms ‘nanoparticles’ and ‘nanomaterial’ have been used for particles of which one representative dimension, for example, diameter of particles on cross-sectional diameter of fibers has at least 100 nm or less. Some people hold that the majority of such fine particles are exhaled without depositing in the respirator tract, and that therefore the particles may not cause pulmonary diseases. However, the properties of nanoparticles are known to be different from the bulk material they are derived from. In cases where the biological effects of bulk materials have been reported, nanosized particles of these materials may be expected to have stronger dose response for the health effects. Every effort must be made to clarify the uncertainty on the risks of these nanomaterials [1]. At the present time, there is no regulation or standard for assessing the biological effects of nanomaterials, and therefore there is a paucity of toxicological data concerning nanomaterials. Much more systematic and strategic studies are needed to enable risk assessments for human health [2–6].

As regards risk assessment and risk management of nanomaterials, the characterization and identification of anticipated risks should be first determined for chemical substances or foods. Conventional assessment methods are applicable for water-soluble particles. For insoluble nanoparticles, the assessment of potential health hazards should be made based on their properties or toxicity and dose–response relationship. The risk is a product of hazard and exposure; even if a nanoparticle has a hazard, the risk is lower when the possibility of exposure to the nanoparticle is small [2].

7.3.2.1 Exposure routes and uptake of nanoparticles

(1) Exposure routes for nanoparticles

Nanoparticles can either be deliberately introduced into the body for medical purposes (drug delivery systems) or absorbed involuntarily from the environment (inhalation of nanoparticle-containing dust in the air). A distinction should also be drawn between nanoparticles manufactured for industrial application and those unintentionally generated and released in the environment, such as welding fumes or diesel exhaust particles (DEP). In the fields of environmental science and toxicology, numerous studies on the potential health hazards caused by ultrafine particles have been conducted. Practically, there are several definitions of nanoparticles or ultrafine particles, however, findings regarding biological effects of the ultrafine particles are useful as a starting point for estimating the effects of nanoparticles on human health.

Human and animals contact with nanoparticles through various routes: nanoparticles can be inhaled in the air, swallowed in the water, ingested in food, and absorbed via the skin in cosmetics. For successful risk assessment, it is important to determine how nanomaterials or nanoparticles are used, such as composites, surface coating, or powders. Coatings or powders have the potential to release a part of their nanomaterials into the environment. Workers who come into contact with nanomaterials have the possibility of exposure to nanoparticles at the workplace. Consumers of products using nanotechnology can also be exposed to them. Attention needs to be paid to the environments and ecosystems in which nanoparticles and nanomaterials are released. Nanoparticles in the products may change their size, quantity, and composition during their life-cycle of manufacturing, use, transportation, and disposal.

(2) Respiratory uptake of nanoparticles

Inhalation is the main route of exposure to nanoparticles. Particles inhaled with the air through the mouth and nose pass through the throat (nasopharynx and oropharynx) and tracheobronchial tree before reaching the alveolar region where oxygen moves from the alveoli to the blood and carbon dioxide moves from the blood to the alveoli. How deeply particles can penetrate and where they become deposited on each respiratory airway such as the nasal cavity, tracheobronchial tree, and the alveoli depend on their size under the various deposition mechanisms: inertial impaction, gravitational sedimentation and diffusion, etc. The respiratory airway includes the anterior nasal passage, posterior nasal passage, pharynx, larynx, trachea, main bronchi, bronchi, bronchioles, terminal bronchioles, alveolar duct, and alveoli, as shown in Fig. 7.3.2. In the human lungs, the trachea divides asymmetrically into the right main bronchus that enters the right lung where it divides into three lobes, that is, an upper, a middle, and a lower, and the left main bronchus that enters the left lung where it divides into two lobes, that is, an upper and a lower. The trachea divides into two branches, dividing progressively to the terminal alveolus.

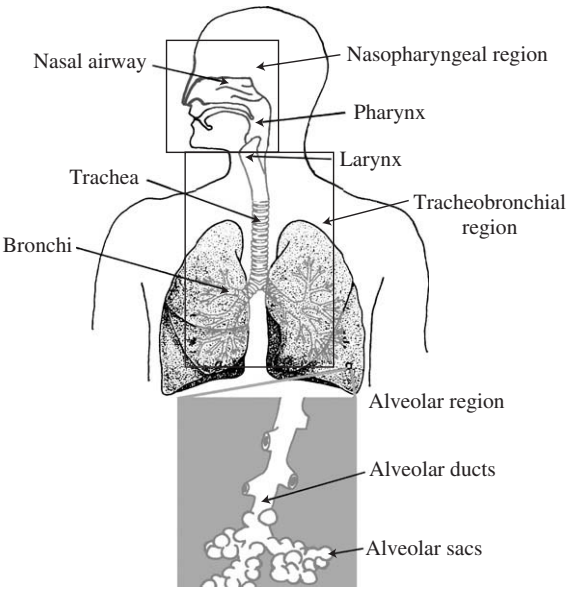

Figure 7.3.2
Anatomical overview of human respiratory tract showing major structures.

To quantitatively assess the pulmonary particle deposition needs human lung morphology models, respiratory physiology based models of the entire lung airway system and aerosol deposition models based on many experimental findings. In 1994, the ICRP Task Group on Lung Dynamic (ICRP: the International Commission of Radiological Protection) published their revised lung model [7]. The deposition, clearance, and translocation of particles in each of the compartments were described. While the model has been widely used in the nuclear field, it is applicable to conventional aerosols as well as radioactive aerosol. In the nuclear field, aerosols including radon progeny that used to be nanoparticles have been studied. Fig. 7.3.3 shows the deposition fractions of inhaled particles per adult nasal respiration of 1.2 m^3/h in each region re-calculated for the nasopharynx, tracheobronchial, and the pulmonary (alveolar) region based on the model. Inhaled aerosol particles deposit on different regions depending on their size; for example, nanoparticles larger than 10 nm deposit mostly in the alveoli and those less than 10 nm deposit in the nasal cavity. How deeply particles penetrate into the lung depends on their size. Nanoparticles can reach pulmonary region in the lung and deposit more intensively and this, therefore, has become one of the reasons for concern about the effects of nanoparticles on human health. However,

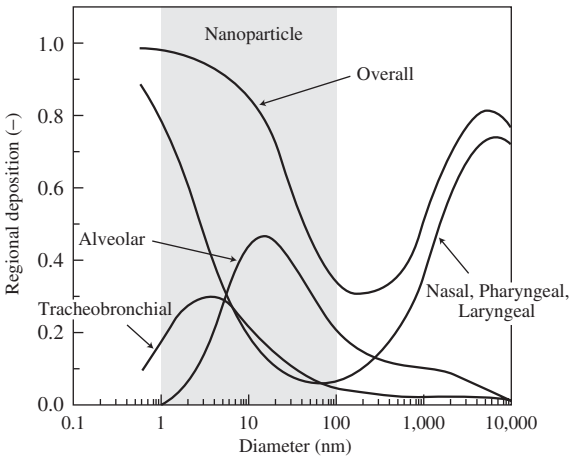

Figure 7.3.3
Predicted fractional deposition of inhaled particles in the nasopharyngeal, tracheobronchial and alveolar region of human respiratory tract during nose breathing based on ICRP Publication 66 [7] (Healthy adult and breathing rate is 1.2 m^3/h).

deposition of nanoparticle chain-like agglomeration and fibrous particles such as carbon nanotubes cannot be estimated by this model.

Most inhaled nanoparticles are deposited on the surface of the respiratory tract. Generally, if insoluble particles are deposited in the ciliated airspaces which are lined with a mucous layer, they are transported to the digestive tract with the mucous flow by mucociliary movements. Particles deposited on nonciliated bronchioles and alveoli are phagocytosed by macrophages, which is a kind of white blood cell. As a result, their residence time is longer, however, they are usually transported to the ciliated upper part of the respiratory tract. Removal of deposited particles described above is called clearance. When the amount of deposited particles is below a certain value, no health effect is produced. In relation to a macrophage response to particles, crystalline silica is hazardous, whereas titanium dioxide is not. Pneumoconiosis is a well-known lung disease that is caused by exposure to dust particles of several micrometers in diameter. Silicosis is a typical form of pneumoconiosis resulting from exposure to crystalline silica dust and characterized by a progressive fibrosis of the lungs. The macrophage-mediated clearance (phagocytes) was effective for micron and submicron particles. It has been reported that only 20% of deposited nanoparticles were removed by the clearance mechanism [8]. It has been suggested that the remaining nanoparticles may pass through the alveolar walls, penetrate into the blood or lymphatic circulation, and be transported to other organs. Many studies have shown that the smaller the particle size the greater the mobility or they pass easily through the alveolar wall and enter into the bloodstream. It is further presumed that the mechanism of health effects of nanoparticles on cardiovascular system other than the respiratory tract is similar to that in the airborne ultrafine particles from DEP.

7.3.2.2 Biological effects of nanoparticles

(1) Biological effects of particulate matters

In Japan, two reference values, the 'administrative control levels' (ACL) and the 'occupational exposure limits' (OELs), are used for the regulation of hazardous chemicals as well as dust (particle matters). OELs are recommended and revised every year by the Japan Society for Occupational Health. OEL (OEL-Mean) for mean concentration of a chemical substance is defined as the reference value to the mean exposure concentration at or below which adverse health effects caused by the substance do not appear in most workers working for 8 h a day, 40 h a week under a moderate workload [9]. The 'threshold limit value' (TLV) has the same definition (but may not be the same values as OEL of the same substance) provided by the American Conference of Governmental Industrial Hygienists (ACGIH).

ACL is an index to determine the control class to judge the propriety of the working environment control based on the results for working environment measurement, which have been implemented for the unit work area in accordance with the Working Environment Measurement Standard. The results of working environment measurement are evaluated by classifying the working environments concerned into three control classes (Control Class I, II, and III). These classes are used as the standards to classify the level of the working environment concerned. Among those subject to working environment measurement, these standards apply to workplace where dust, lead, organic solvent, and specified chemical substances are used. Article 65 of the Industrial Safety and Health Law stipulates that certain workplaces in which harmful substances are involved or harmful work operations are performed shall be the subject to working environment measurement. A 50% cut-off size of the dust particle is set at 4 μm for both standards and is far larger than nanosized particles. OEL or ACL [10] for particulate matters are usually based on mass concentration, that is, milligram per cubic meter. Therefore, if the particulate matters have broad size distribution, the contribution of nanoparticles is not large to in terms of mass of particles.

Evidence from a number of toxicological studies on insoluble particles indicates that the primary determinant of the health effect of particles depends on the surface area of particles deposited [11, 12]. On the basis of the results from a number of in vitro studies of insoluble nanoparticles, a hypothetical cellular interaction has been proposed [13]: inflammation and oxidative stress can be mediated by several primary pathways: (1) the particle surface causes oxidative

stress resulting in increased intracellular calcium and gene activation; (2) transition metals released from particles result in oxidative stress, increased intracellular calcium, and gene activation; (3) cell surface receptors are activated by transition metals released from particles, resulting in subsequent gene activation; or (4) intracellular distribution of insoluble nanoparticles to mitochondria generates oxidative stress.

In the workplace, the concentration of nanoparticles may be at a high level and most of the nanoparticles become agglomerates, while nanoparticles will form single nanoparticle at low levels in the general environment. It is a matter of debate whether agglomerates of nanoparticles react as a larger particle or a single nanoparticle in the lung or other organs.

If insoluble particles are retained in the lung for a longer time without enough clearance mechanisms, they can cause pulmonary inflammation or pneumoconiosis. It is of interest that nanoparticles deposited in the lung can move into the blood vessel through alveolar epithelium and they can damage vessels or produce blood clots [14, 15]. In a recent study, nanoparticles deposited in the nose may move directly to the brain via the olfactory bulb [16].

(2) Biological effects of fullerene

The biological effects of fullerene have being investigated intensively. In rats dosed orally with radioisotope-labeled C_{60} fullerenes, most were excreted in the feces and some were found in the urine. A small amount of them can be absorbed via the gastrointestinal tract. In contrast, in the same study, 90% of the same labeled fullerenes administered intravenously were retained after 1 week, with most found in the liver [17].

LD50s (acute toxicity) by intraperitoneal injection in mice and rats were 1.2 and 0.6 g/kg, respectively. The dose of 2.5 g/kg orally in rats did not result in death. The reproductive translocation of fullerenes was also observed in mice. Fullerenes have shown mutagenic activity in Ames tests. Fullerenes have shown no skin irritation or allergic reactions [18].

On the other hand, fullerenes are being tested for possible medical use. Fullerenes are basically hydrophobic but water-soluble derivatives have been synthesized to be used as drugs or its carrier. The derivative can be anticipated as drugs, for example, anti-AIDS drug. It has been stated that the toxicity of fullerenes changes due to slight structural changes including chemical modification [18].

(3) Biological effects of carbon nanotubes

Carbon nanotubes are chemically stable and are similar in form and size to asbestos; these characteristics have given rise to concern that carbon nanotubes may have the potential to cause pulmonary diseases such as lung cancer and mesothelioma similar to asbestos. A few data are available concerning the biological effects of carbon nanotubes. The biological effects of carbon nanotubes are being researched. Epithelioid granulomas and interstitial inflammation are induced in mice and rats following exposure to single-walled carbon nanotubes [18–20]. Untreated carbon nanotubes contain the nanoparticles of transition metals such as iron and nickel, which are used as catalysts in forming carbon nanotubes. These nickel-containing carbon nanotubes have been reported to be toxic [19].

The concentration of airborne asbestos fibers is expressed as a number concentration, that is, fibres per cubic centimeter or fiber per liter. When fiber concentrations are determined by phase contrast light microscopy, the fibers with a diameter of less than 3 μm, a length longer than 5 μm, and a length-to-diameter ratio (aspect ratio) greater than 3 are counted [21]. Asbestos fibers having nanosized diameter were often observed in analyses of environmental samples using electron microscopy. International Agency for Research on Cancer (IARC) rated asbestos as a known human carcinogen (group 1) [22] and the concentration of chrysotile asbestos is expressed as a risk level of 0.15 fiber/cm^3 [9]. Health effects of vitreous fibers and other asbestos substitutes have been assessed to determine their OELs or their carcinogenicity in humans. The health effects of carbon nanotubes are being intensively investigated now.

(4) Biological effects of carbon black

The OEL for carbon black respirable dust is 1 mg/m^3 and these for activated charcoal and graphite are 0.5 mg/m^3 in each [9]. In the Ref. [23], while rats and mice inhaled carbon black with a particle diameter of ~30 nm at a concentration of 5–13 mg/m^3 did not produce any specific changes, particles (agglomerate of small particles) of ~450 nm at a concentration of 2–6 mg/m^3 produced early pulmonary changes.

(5) Biological effects of metal oxides

Micronsized titanium dioxide particles are thought to have almost no toxicity and often used as a negative control substance. The OEL for titanium dioxide is 1 mg/m^3 for respirable fraction [9]. However, the results of a series of studies by Oberdörster et al. [3, 11, 24, 25] on submicron- and nanosized titanium dioxide suggested that as size decreases, inflammatory effects are intensified, and normally nontoxic substances may assume hazardous characteristics. Fig. 7.3.4 shows a part of the results by Oberdörster et al. in which rats and mice were exposed to anatase titanium dioxide particles [25]. Their results have been frequently cited in the discussion of whether the health effects of fine particles should be based on its mass or its surface area. In Fig. 7.3.4, percentages of neutrophils in lung lavage of rats are shown as indicators of inflammation after intratracheal instillation

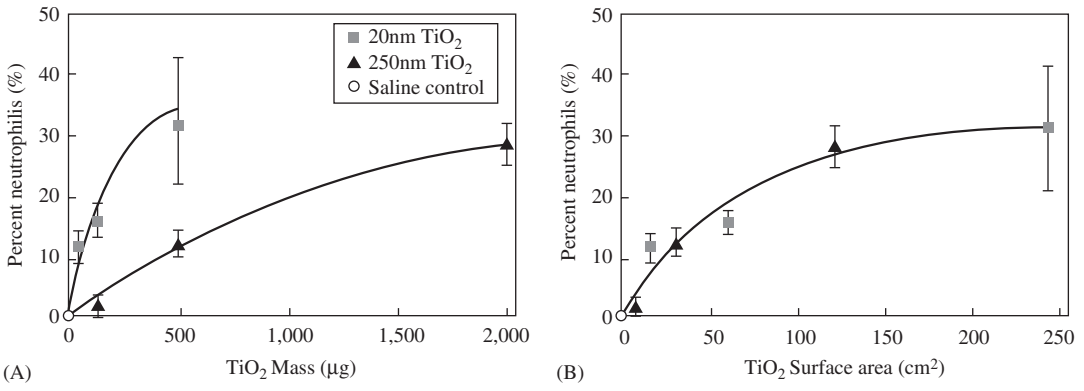

Figure 7.3.4
Percentage of neutrophils in lung lavage of rats as indicators of inflammation 24 h after intratracheal instillation of different mass doses of 20 and 250−nm TiO_2 particles in rats [3]. (A) The dose responses of two samples are different from each other as mass. (B) The same response relationship is shown as particle surface area.

of different mass doses of 20 and 250 nm TiO_2 particles. The steeper dose response of nanosized TiO_2 particles is observed than for submicron TiO_2 particles when the dose is expressed as mass (Fig. 7.3.4A). If the same dose–response relationship as in Fig.7.3.4A is indicated as particle surface area (Fig. 7.3.4B), the particle surface area seems to be a more appropriate dosimetric for comparing effects of different-sized particles of the same chemical structure.

Zinc oxide is a white powder and used in pigments. The OEL is 1 mg/m^3 for its respirable fraction [9], and the value for zinc oxide fume which causes metal fume fever is under consideration.

Nanoparticles of transition metals and rare earth elements and their oxides will be used widely. Since many of these metals and their oxides have biological effects, particular attention should be given to them.

Nickel compounds are rated as a human carcinogen (group 1) by IARC. In particular, nickel oxide is particularly insoluble among the nickel compounds and remains longer in the lung. Nanosized nickel oxide particles have greater toxicity to the lung than larger particles [26, 27]. Pulmonary inflammatory responses induced by nanosized cobalt particles have been reported [28–30]. Biological effects of nanosized particles of other transient metals such as iron and manganese have received attention [3].

Rare earth elements are a general term of 17 chemical elements consisting of scandium (Sc), yttrium (Y), and a lanthanide series of 15 elements from lanthanum (La) to lutetium (Lu). These elements have been used in magnetic alloy, fluorescent and hydrogen storage alloy. Particularly cerium oxide nanoparticles are frequently used as a fuel additive and are incorporated in cosmetics formulation. The potential biological and environmental effects of these elements have not sufficiently been investigated. It has been demonstrated that LD50s for these elements in oral and intravenous administration are in a range from several dozens to several thousands milligrams per kilograms, indicating that none of these elements has high toxicity. In the results of studies in which the biopersistence and the distribution of rare earth compounds in the body were investigated, for example, the compounds deposited in bones and teeth, and organs including lung, liver, spleen and kidney following intratracheal, oral, intravenous, and intraperitoneal administration. Although the compounds deposited predominantly in the liver other than bones, it has also been reported that the distribution of the compounds in the lung and spleen increased when the dose was increased [31].

The demand for indium compounds has been sharply increasing. The compounds have been used in the materials for transparent electrodes for flat panel displays. In Japan, the cases of pulmonary interstitial pneumonia and pulmonary fibrosis have been reported in workers engaged in cutting and grinding of sintered indium–tin oxide (ITO) and potentially having inhaled the dusts released from ITO [32, 33]. The biological effects of indium arsenic compounds and indium phosphorus compounds also have been investigated. The ACGIH has proposed a value of 0.1 mg/m^3 for their TLV, and the value has been applied tentatively in Japan.

References

[1] The Royal Society, *Nanoscience and Nanotechnologies:* ISBN 0 85403 604 0, http://www.nanotec.org.uk/finalReport.htm (2004).

[2] M. Takemura: *ChemoBio Integr. Manage.*, **1**, 57–73 (2005) (in Japanese).

[3] G. Oberdörster, E. Oberdörster and J. Oberdörster: Nano-toxicology: *Environ. Health Perspect.*, **113**, 823–840 (2005).
[4] P. Biswas, C.Y. Wu: *J. Air Waste Manage. Assoc.*, **55**, 708–746 (2005).
[5] A.D. Maynard, E.D. Kuempel: *J. Nanoparticle Res.*, **7**, 587–614 (2005).
[6] K. Thomas, P. Sayre: *Toxicol. Sci.*, **87**, 316–321 (2005).
[7] International Commission on Radiological Protection. Publication 66: *Ann. ICRP* **24**, 1–300 (1994).
[8] J. Ferin, G. Oberdörster, S.C. Soderholm and R. Gelein: *J. Aerosol Med.*, **4**(1), 57–68 (1991).
[9] Recommendation of Occupational Exposure Limits: *J. Occup. Health*, **48**(4), 296 (2005).
[10] Ministry of Health, Labor and Welfare, Japan. Notification 368, Working Environment Evaluation Standards (2004).
[11] G. Oberdörster, J. Ferin, R. Gelein, S.C. Soderholm, J. Finkelstein: *Environ. Health Perspect.*, **97**, 193–197 (1992).
[12] K. Donaldson, X.Y. Li, W. MacNee: *J. Aerosol Sci.*, **29**, 553–560 (1998).
[13] K. Donaldson, C.-L. Tran: *Inhal. Toxicol.*, **14**, 5–27 (2002).
[14] A. Nemmar, M.F. Hoylaerts, P.H.M. Hoet, D. Dinsdale, T. Smith and H. Xu, J. Vermylen, B. Nemery: *Am. J. Respir. Crit. Care Med.*, **166**, 998–1004 (2002).
[15] A. Nemmar, M.F. Hoylaerts, P.H.M. Hoet, J. Vermylen and B. Nemery: *Toxicol. Appl. Pharmacol.*, **186**, 38–45 (2003).
[16] G. Oberdörster Z. Sharp, V. Atudorei, A. Elder, R. Gelein and W. Kreyling, C. Cox: *Inhal. Toxicol.*, **16**(6/7), 437–445 (2004).
[17] S. Yamago, H. Tokuyama, E. Nakamura, K. Kikuchi, S. Kananishi, K. Sueki, H. Nakahara, S. Enomoto, F. Ambe: *Chem. Biol.*, **2**, 385–389 (1995).
[18] Y. Ishihara, R. Sakata and Y. Fujita: *J. Aerosol Res.*, **20**, 193–199 (2005) (in Japanese).
[19] C.W. Lam, J.T. James, R. McCluskey, R.L. Hunter: *Toxicol. Sci*., **77**, 126–134 (2004).
[20] D.B. Warheit, B.R. Laurence, K.L. Reed, D.H. Roach, G.A.M. Reynolds, T.R. Webb: *Toxicol. Sci.*, **77**, 117–125 (2004).
[21] WHO: Environmental Health Series 4. World Health Organization, Copenhagen (1985).
[22] IARC (International Agency for Research on Cancer): *IARC Monogr. Eval. Carcinog. Risks Hum.*, **81**, 1–418 (2002).
[23] J.H.E. Arts, S.M. Spoor, H. Muijser: *Inhal. Toxicol.*, **12**, 261–266 (2000).
[24] G. Oberdörster, J. Ferin, J. Finkelstein, P. Wade and N. Corson: *J. Aerosol Sci.*, **21**, 384–387 (1990).
[25] G. Oberdörster: *Philos. Trans. R. Soc. Lond. A*, **358**, 2719–2740 (2000).
[26] A. Ogami, M. Hirohashi, Y. Nagafuchi, K. Kuroda: *J. Aerosol Res.*, **20**, 200–206 (2005) (in Japanese).
[27] IARC (International Agency for Research on Cancer): Summaries & Evaluations – Nickel and Nickel Compounds, Lyon, France, Vol. 49 (1990).
[28] Q. Zhang, Y. Kusaka: *Inhal. Toxicol.*, **12**, 267–273 (2000).
[29] Q. Zhang, Y. Kusaka and K. Donaldson: *J. Occup. Health*, **42**, 179–184 (2000).
[30] Q. Zhang, Y. Kusaka, X. Zhu, K. Sato, Y. Mo, T. Klutz and K. Donaldson: *J. Occup. Health,* **45**, 23–30 (2003).
[31] M. Takaya, T. Toya, A. Takata, N. Otaki, K. Yoshida and N. Kohyama: *J. Aerosol Res.*, **20**, 207–212 (2005) (in Japanese).
[32] A. Tanaka: *J. Aerosol Res.*, **20**, 213–218 (2005) (in Japanese).
[33] A. Tanaka, M. Hirata, M. Omura, N. Inoue, T. Ueno, T. Homma, K. Sekizawa: *J. Occup. Health*, **44**, 99–102. (2002)

7.3.3 Safety assessment for the nanoparticles

We have been experiencing amazing progress of the technology on the processing for the nanometer-sized materials. The applications cover even biomedical engineering in addition to information technology, material, environmental science, and energy production [1–5]. As the result, many kinds of new materials have been designed, fabricated, and discarded. From now on, this movement will be accelerated and even more new functional materials will be distributed in the world. Here, we should not forget the safety of those materials in the process of the production, usage, and discard. Without this safety assessment, we will go into the same problems as that of asbestos just we are facing now. First of all, we have to conduct experiments to reveal the minimal concentration for emergence of the toxicity. In other words, we have to fix the standard value for the threshold concentration for each material first of all. If we do not fix it, we should not use the material at any concentration, which means any engineering process could not be carried out. The applications in the various fields have started all over the world, and the safety assessment is urgently needed. In this article, we introduce the methods of the safety assessment of the semiconductor nanoparticles and describe the safety and the threshold depending on the surface treatment.

The production process and the surface treatment play one of the most important roles for the safety of the nanoparticles. Cd and Se semiconductor nanoparticles coated with ZnS are one of the most widely used for the strong intensity of the fluorescent activity. Cd oxide and Se compounds once dispersed in the tri-octhil-phosphine oxide (TOPO) heated up to 300°C generate nanoparticles by self-assembly. Then ZnS

enhances the stability of the structure and raises up the fluorescent intensity than without the coated one.

Nanoparticles, thus manufactured, as materials for a novel memory in the field of intelligence technology (IT), and as super-micro devices for laser in the field of optics, have been developed all over the world [1–5]. These nanoparticles cannot be dissolved into water, but dissolved into organic solvents like toluene. Therefore, for biological and medical applications, various technologies for surface-conjugations to make them hydrophilic [6, 7] have been developed. For example, nanoparticles covered with TOPO are hydrophobic because an alkyl group on them is hydrophobic. Therefore, a technology for replacing this alkyl group with hydrophilic carbonic acid (making the whole particles soluble in water) has been developed [6].

Nanoparticles, thus surface-treated, can be dissolved into water, like sodium salt or potassium salt. With this method, various kinds of materials have been surface-conjugated.

7.3.3.1 The MTT assay method and thresholds for cyto-toxicity

The MTT assay method is a way to evaluate the hazard assessment of nanoparticles, in which the activation metabolism in a mitochondrium in a cell is measured and the influence of nanoparticles on the prolification of the cell is qualitified. The MTT is a kind of tetrazolium, whose molecular formula is $C_{18}H_{16}BrN_5S$. Taken into a cell, it is decomposed by a dehydrogenase enzyme in a mitochondrium into a pigment called 'hormazan'. The measurement of the fluorescence intensity of the pigment shows the prolification of the cell [8–10].

Fig. 7.3.5. shows the hazard assessment of Vero cells and kidney cells of the African Green Monkey against CdSe/ZnS nanoparticles. The horizontal axis shows the concentrations of the nanoparticles and the vertical axis the fluorescence intensity of the hormazan at 460 nm, that is, the metabolism of the cells. The figure indicates

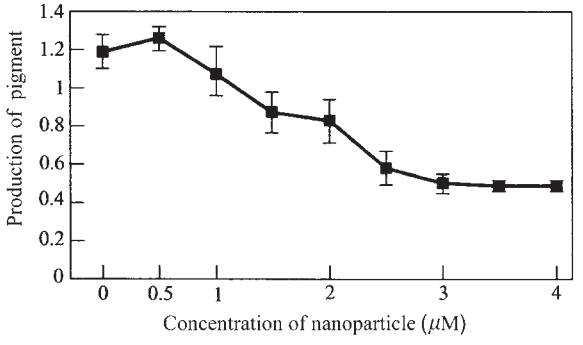

Figure 7.3.5
Cyto-toxicity of the quantum dots by the MTT assay.

that cyto-toxicity is not observed for 10^5 cells when the concentration is less than 0.5 μM. This result means that this concentration is the threshold of the cell toxicity. Likewise, cyto-toxicity is not observed for the HeLa cells and for the human primary cells. Further, in order to find out how the sizes of nanoparticles influence the cyto-toxicity, the cyto-toxicities were evaluated with three kinds of quantum dots; one whose fluorescence wavelength is 640 nm, red, one with 570 nm, yellow, and the other with 520 nm, green. The following results were obtained. The largest quantum dots whose fluorescence wavelength is 640 nm show a tendency to give cyto-toxicity. Cyto-toxicity is observed at concentrations more than 1 μM [11].

7.3.3.2 Measurement of cyto-toxicity by the flow cytometry

Another method to evaluate cyto-toxicity is the flow cytometry [12]. The MTT assay alone cannot tell whether the toxicity observed is lethal to the cells or just restrains the prolification of them. In the flow cytometry, the nuclei of dead cells are dyed with propidium iodide (PI) after the nanoparticles are taken in and the ratios of the dead cells are measured. Fig. 7.3.6 shows the lethal cyto-toxicity of MUA conjugated nanoparticles (520 nm, green) against Vero cells. The vertical axis indicates the numbers of the cells, and the horizontal axes show the fluorescence intensities and the cyto-toxicities. These experiments also show that dead cells cannot be observed at concentrations less than 0.5 μM even though nanoparticles are taken in, as was shown in the MTT assay. However, at concentrations more than 2 μM, the nanoparticles taken in cause damage to more than the half of the cells. That is, the cyto-toxicity of MUA quantum dots against cells is lethal [11].

7.3.3.3 Relations between surface-conjugations of nanoparticles and their safety

Nanoparticles have been surface-conjugated for applications for various uses.

Some surface-conjugations cause more grave cyto-toxicity than others. Therefore, relations between surface-conjugations and their safety for cells have to be considered. In order to find out the relations, the safety evaluations of nanoparticles surface-conjugated with two materials were made; one is with MUA (quantum dots-COOH) and the other is with glycerol (quantum dots-OH), and their purified and unpurified particles. Fig. 7.3.7 shows that the purification reduces the cyto-toxicity for the quantum dots-OH, and that the toxicity remains the same after the purification for the quantum dots-COOH. MUA itself, a material with which particles are conjugated, has cyto-toxicity. This experiment shows that toxicity against cells is connected not only with particles themselves but also with kinds of surface-conjugations and degrees of purification.

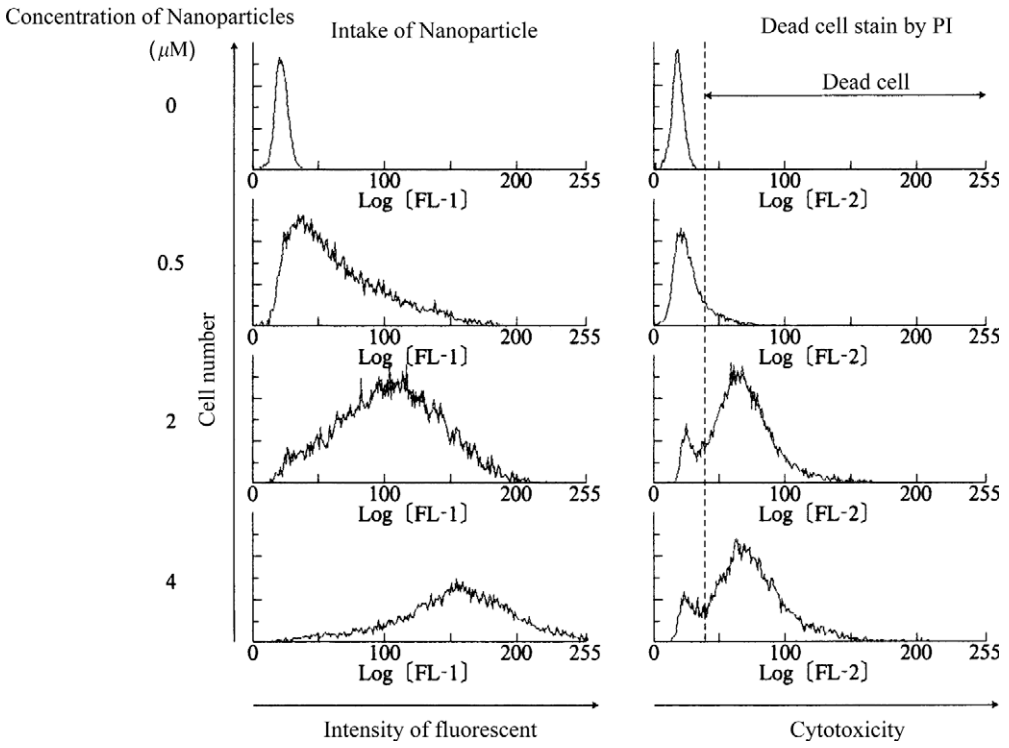

Figure 7.3.6
The detection of cyto-toxicity with flow cytometry.

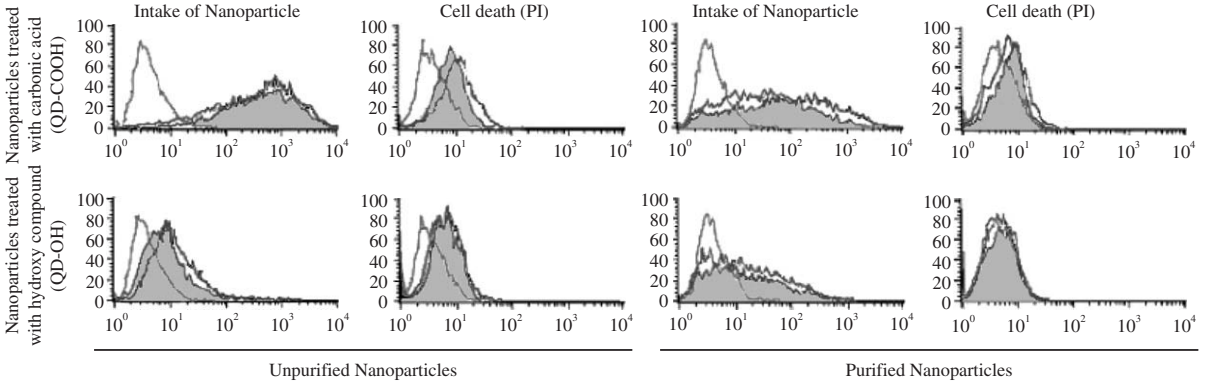

Figure 7.3.7
Differences of surface-conjugations and their cyto-toxicities.

7.3.3.4 Quantitative evaluation of damaged DNA; the comet assay

It is shown in the above experiments that the toxicity of nanoparticles is lethal to cells. Next, we found out by the Comet Assay method whether the toxicity is derived from damaged DNA. The method is a way to evaluate quantitative damage of DNA by electrophoresis. The fragmented DNA seeps out of their cells by treating cells, whose DNA has been fragmented, with agarose-gel to break their cell membrane, and then electrophoresing them. It looks like the "tales of comets". Cells, whose DNA has not been fragmented, have their nuclei keeping their spherical

shape after electrophoresis, and the tales of comets cannot be observed [13–16].

Fig. 7.3.8 shows the results of the experiments with quantum dots conjugated with COOH (both purified and unpurified) to WTK-1 cells, a human lymphoblast mutation strain [17]. The vertical axis shows the lengths of the tails, and the horizontal axis the concentrations of the quantum dots. The concentration of the nanoparticles is 2 μM.

The results are as follows: the unpurified quantum dots with COOH caused damage to DNA. On the other hand, the electrophoresis with the purified quantum dots does not show DNA damage. This is probably because the DNA damage has been repaired during the longer cultivation time.

Fig. 7.3.9 shows the results of DNA damage. The nanoparticles have been purified over and over again in order to get rid of impurities derived from the process of the surface-conjugation. The concentrations are from 0.5 to 2 μM for 10^5 cells. The cultivation time after the addition of the nanoparticles is 24 h. Hydrogen peroxide (aqua) is used as the positive control. The results show; DNA damage is not observed up to 2 μM. The same experiment was

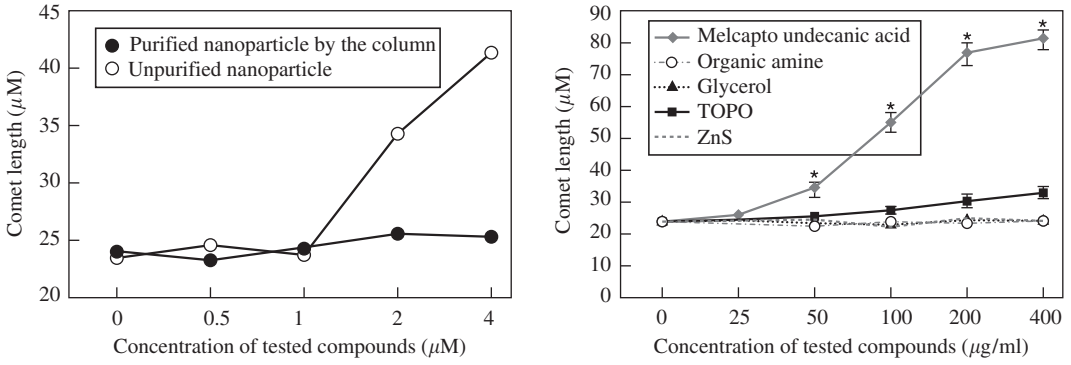

Figure 7.3.8
Cyto-toxicity of nanoparticles by the Comet Assay.

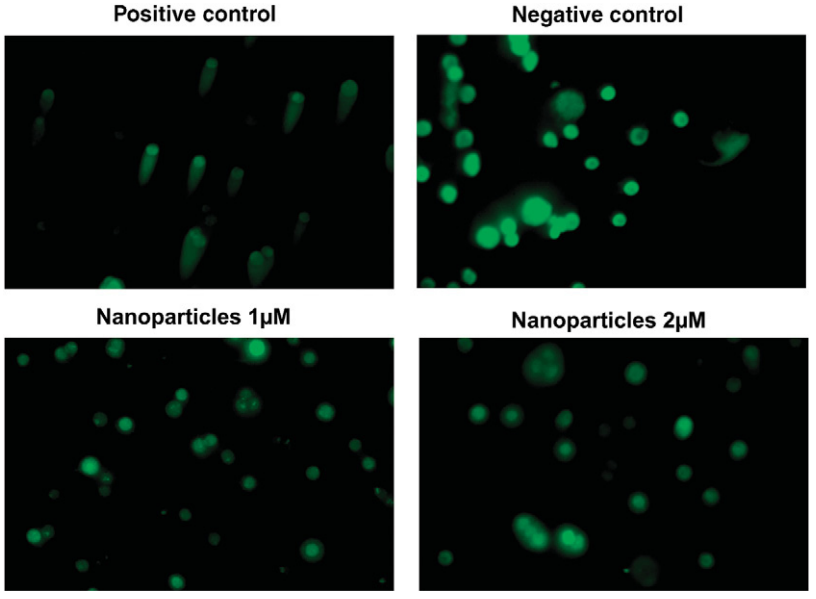

Figure 7.3.9
Microscopic study for the Comet Asssay and the estimation of the cyto-toxicity.

conducted with quantum dots conjugated with MUA, and quantum dots-NH_2 with an amino group. DNA damage was not observed in either case. The results indicate that as far as particles themselves do not break down, the cyto-toxicity of quantum dots is derived from the chemical properties of the materials covering the quantum dots.

The safety evaluation of nanoparticles has not been conducted sufficiently. As indicated above, the procedure for surface-conjugation could apply not only to Cd/Se nanoparticles but also to other nanoparticles. Today, various kinds of techniques for surface-conjugations have been available in academic papers, proceedings, and on the Internet. Some of them are widely known and others are patented. Those techniques are all shared among the human race.

Even at this moment, the human beings are making breakthroughs in various fields and developing different kinds of technologies. Sharing these technologies will lead to still more speedy developments of yet more advanced technologies. To achieve it, these technologies should be so structured that different fields, for example, bioimaging and biotechnology, structured on their own, can be linked to each other. Such structured knowledge will play an essential part in merging different fields.

References

[1] S. Coe, W.K. Woo, M. Bawendi and V. Bulovic: *Nature*, **420**, 800–803 (2002).

[2] T.C. Harman, P.J. Taylor, M.P. Walsh and B.E. LaForge: *Science*, **297**, 2229–2232 (2002).

[3] C. Santori, D. Fattal, J. Vuckovic, G.S. Solomon and Y. Yamamoto: *Nature*, **419**, 594–597 (2002).

[4] X. Li, Y. Wu, D.Y. Steel, D. Gammon, T.H. Stievater, D.S. Katzer, D. Park, C. Piermarocchi and L.J. Sham: *Science*, **301**, 809–811 (2003).

[5] A. Zrenner, E. Beham, S. Stufler, F. Findeis, M. Bichler and G. Abstreiter: *Nature*, **418**, 612–614 (2002).

[6] W.C. Chan, S. Nie: *Science*, **281**, 2016–2018 (1998).

[7] K. Hanaki, A. Momo, T. Oku, A. Komoto, S. Maenosono, Y. Yamaguchi and K. Yamamoto: *Biochem. Biophy. Res. Commun.*, **302**, 496–501 (2003).

[8] M. Ishiyama, Y. Miyazono, K. Sasamoto, Y. Ohkura and K. Ueno: *Talanta*, **44**, 1299 (1997).

[9] T. Mosman: Rapid colorimetric assay for cellular growth and survival: *J. Immunol. Method.*, **65**, 55–63 (1983).

[10] H. Tominaga, M. Ishiyama, F. Ohseto, K. Sasamoto, T. Hamamoto, K. Suzuki and M. Watanabe: *Anal. Commun.*, **36**, 47 (1999).

[11] A. Shiohara, A. Hoshino, K. Hanaki, K. Suzuki and K. Yamamoto: *Microbiol. Immunol.*, **48**, 669–675 (2004).

[12] A.N. Shatrova, N.D. Aksenov, A.I. Poletaev, V.V. Zenin: *Tsitologiia*, **45**(1), 59–68 (2003).

[13] H. Hoffmann, G. Speit: *Mutat. Res*. **581**(1–2), 105–114 (2005).

[14] S. Lemiere, C. Cossu-Leguille, A.M. Charissou and P. Vasseur: *Biomarkers*, **10**(1), 41–57 (2005).

[15] F. Mattiolo, A. Martelli, C. Garbero, M. Gosmar, V. Manfredi, F.P. Mattiolo, G. Torre and G. Brambilla: *Toxicol. Appl. Pharmacol.*, **203**(2), 99–105 (2005).

[16] F. Mouchet, L. Gauthier, C. Mailhes, M.J. Jourdain, V. Ferrier and A. Devaux: *J. Toxicol. Environ. Health A*, **68**(10), 811–832 (2005).

[17] A. Hoshino, K. Fujioka, T. Oku, M. Suga, Y. F. Sasaki, T. Ohta, M. Yasuhara, K. Suzuki and K. Yamamoto: *Nano Lett.*, **4**(11), 2163–2169 (2004).

7.4 Removal of nanoparticles

7.4.1 Principle of particle removal

In order to prevent nanoparticles release from a system so as to maintain environmental safety, the removal technique of nanoparticles must be established. In this section, separation techniques of particles from exhausted or suspended gas and liquid are described focusing on particles less than 100 nm.

Generally, as shown in Fig. 7.4.1, all particle separators for a dispersed system employ either one of three basic forms of particle separation. On the left hand side of the figure lie the separation methods in which particles are collected only by force field (electrostatic force, centrifugal force, gravity force, etc.), and the representative separator is electrostatic precipitator (ESP). If some obstacles (collectors) are placed into the particle laden stream, particle separation is facilitated because particles are collected on obstacles with a smaller deviation from the fluid flow by the force exerting on the particles compared to the case without obstacles. Typical collectors of this form are air filter, deep bed filter, etc. On the right hand side of the figure lie separators that collect particles utilizing only sieving effect of obstacles without any force field. In this case, geometrical size of channel between the obstacles must be smaller than that of particles. Membrane filter, fabric filter, etc. belong to this group.

When we apply the above collection forms to nanoparticles, the major collection mechanisms are Brownian diffusion and electrostatic force for particles in gas, while sieving effect and interception/adhesion forces for those in liquid.

7.4.2 Removal of nanoparticles suspended in gas

As mentioned above, most airborne particles are collected by separators utilizing various kinds of forces such as gravity, centrifugal force, electrostatic forces, inertia, Brownian diffusion force, and so on.

Elementary cause	Force field	Force field and obstacle	Obstacle
Form	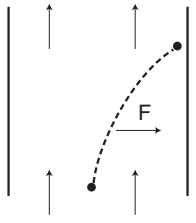	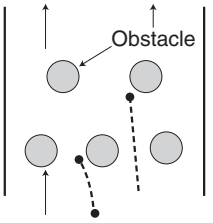	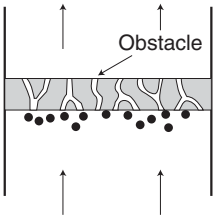
Collection efficiency	low	middle	high
Pressure drop	low	middle	high
Critical factor for performance	• Deposition velocity	• Collision efficiency • Pressure drop	• Pressure drop
Separator	• Thickner • ESP • Cyclone	• Venturi scrubber • Fibrous filter • Granular bed	• Filter press • Bag filter • Membrane filter

Figure 7.4.1
Basic forms of particle separation.

Therefore, the migration velocities or displacement of a particle per second due to the individual forces gives the basis for the comparison of removal efficiencies due to each force. In Fig. 7.4.2, migration velocities of particles due to various forces are depicted against particle diameter at normal temperature and pressure for particle density of 1 g/cm^3 [1]. As seen from the figure, the velocities due to gravity, centrifugal force, and inertia monotonically decrease with decreasing particle diameter, suggesting that the removal of nanoparticles with these forces is difficult. On the contrary, the velocities due to Brownian diffusion and electrostatic forces increase with decreasing particle diameter for particles less than 100 nm. This suggests that Brownian diffusion and electrostatic forces are most effective in collecting nanoparticles.

Fig. 7.4.3 summarizes typical conventional dust collectors. Among them, the effective collectors for nanoparticles are ESP and fabric/air filter. However, for the case of ESP, which relies on only electrostatic force, nanoparticles (< 10 nm) fail to carry even one electron resulting in low collection efficiency. In this case electrically charged filters are effective because we can expect the combined effects of electrostatic forces and Brownian diffusion.

Among charged filters, so-called electret filter, which consists of permanently polarized fibers, is the most favorable filter because of its charge stability. Particle penetration data of electret filter are plotted against particle diameter in Fig. 7.4.4 and compared with that of uncharged filter with the same structure. For the three combinations of charged states of fiber and particle there exist the most penetrating particle

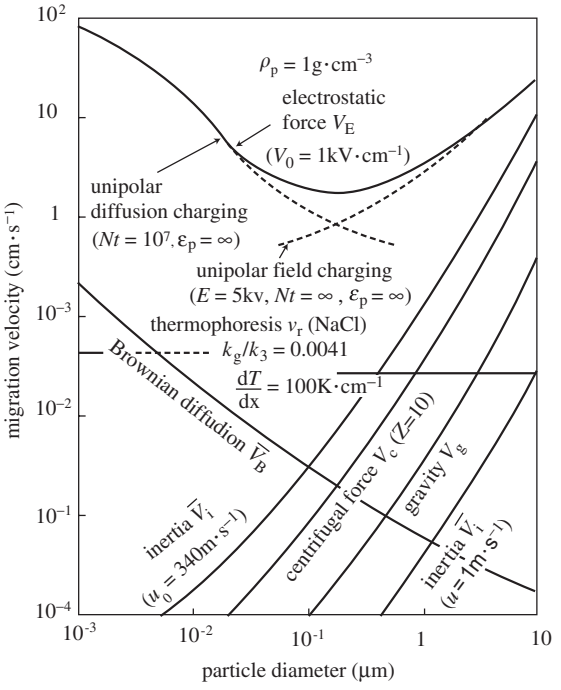

Figure 7.4.2
Migration velocity of airborne particles under force fields.

diameters. For the uncharged fiber, collection efficiency of uncharged particle has a minimum at 100 nm and increases with decreasing particle diameter, showing that 100 nm is the most penetrating

type	typical collector	shape of collector	particle size
gravity	settling chamber	dusty air → clean air	>20 μm
inertia	mist separator	screen	>10 μm
centrifugal force	cyclone		>2 μm
scrubbing	venturi scrubber	nozzle, spray	>0.5 μm
filtration	bag filter	fabric	all size range (high conc.)
	air filter	Fibrous layer	all size range (low conc.)
electrostatic force	electrostatic precipitator (EPS)	discharge electrode, HV, collection electrode	>50 nm

Figure 7.4.3
Classification of particle separators.

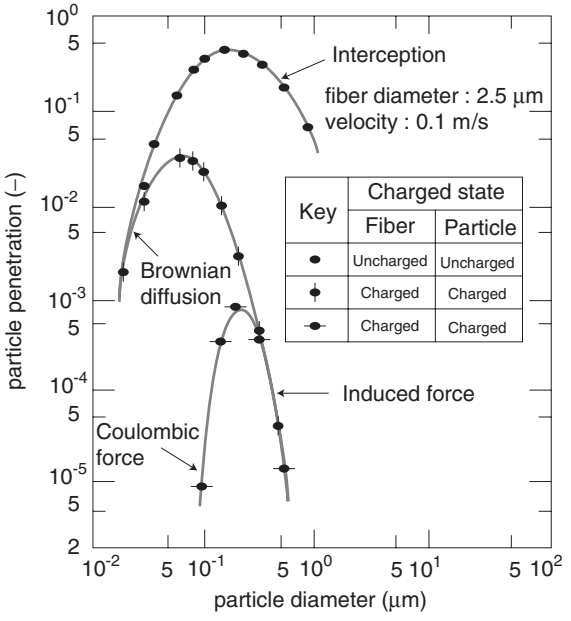

Figure 7.4.4
Particle penetration of electrically charged filter.

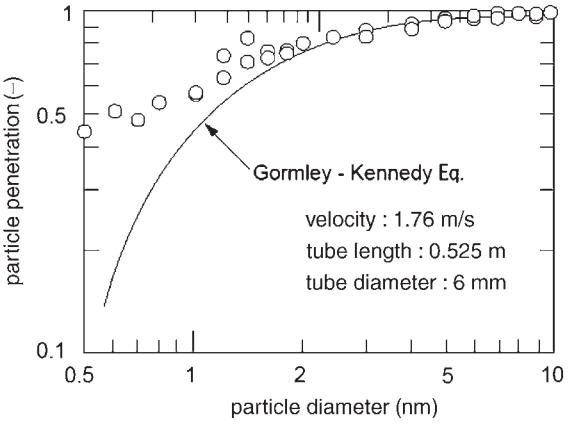

Figure 7.4.5
Penetration of airborne nanoparticles through a circular tube.

particle size. For the charged fiber, particle collection efficiency is very high even for uncharged particle, and the efficiency for charged nanoparticles is extremely high because of strong Coulombic force between fiber and particle. The experimental data plotted in Fig. 7.4.4 are qualitatively in good agreement with the theoretical prediction following the particle size dependency on particle migration velocity (shown in Fig. 7.4.2).

However, as particle size becomes smaller and comparable with the size of a molecule, particles may rebound on a collector surface, and the adhesion probability of particles drops, resulting in a decrease in collection efficiency. Fig. 7.4.5 is an example of experimental data that confirm the particle rebound [2]. The figure shows the penetration of nanoparticles through a grounded circular tube. The solid curve is the theoretical line derived by assuming that particles are deposited from a laminar flow in a tube by Brownian diffusion. It is evident that experimental penetration deviates from the theoretical line for particles less than 2 nm. This means that molecular behavior begins to appear when the particle size becomes as small as 2 nm, and as a result, the collection efficiency is reduced.

It should be noted that considerable amounts of nanosized particles are contained in diesel exhaust particles (DEP), possibly penetrating through the honeycomb type (tubular channel) diesel particulate filters (DPF).

References

[1] K. Takahashi: Ouyou Earozorugaku, Youkendou, p. 144, (1984).

[2] Y. Otani, H. Emi, S.J. Cho and N. Namiki: *Adv. Powder Technol.*, **6**(4), 271–281 (1995).

7.4.3 Removal of nanoparticles in liquid

There are two types of methods that differ in the way the nanoparticles in liquid are collected. The first group, called membrane filtration, constrains the particles by a membrane, and the liquid is allowed to flow freely through the membrane. In the second group of ultracentrifugation, the liquid is constrained in a rotating vessel, and the particles move freely within the liquid by an external field of acceleration caused by ultracentrifugal field. These methods have been quite extensively used in separation of macromolecules and molecules from liquid, and they are recently becoming important also in separation of nanoparticles from liquid.

7.4.3.1 Fouling mechanism in membrane filtration

In pressure-driven membrane filtration processes, the pressure gradient across the membrane would force solvent and smaller species through the pores of the membrane, while the larger molecules/particles would be retained. Membrane filtration processes are usually classified into three general categories according to the size of separating components, as shown in Fig. 7.4.6. Microfiltration (MF) is designed to retain suspended particles in the range of 50 nm–5 μm. Ultrafiltration (UF), on the other hand, retains macromolecules or nanoparticles in the range of 5–50 nm (nominal molecular weight cut-off (NMWCO) ranging from 5,000 to 5,000,000 Da). Nanofiltration (NF) is a relatively new process that uses charged membranes, and it covers molecular sizes ranging from 0.1 to 5 nm (NMWCO ranging from 200 to 1,000). It is useful in that it can separate dissociated forms of a compound from the undissociated form.

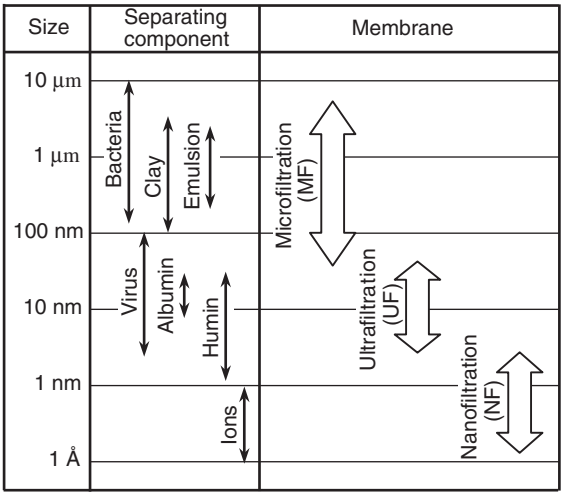

Figure 7.4.6
Useful ranges of various membrane filtration processes.

One of the major factors limiting the use of membrane filtration is membrane fouling, resulting in a dramatic decline in flux with time of operation. To account for the membrane fouling, the resistance-in-series model is frequently employed. The resistance model becomes

$$u_1 = \frac{dv}{d\theta} = \frac{p}{\mu R_t} = \frac{p}{\mu(R_{bm} + R_c + R_{cp})} \qquad (7.4.1)$$

where u_1 is the permeate flux, v the filtrate volume per unit membrane area, θ the filtration time, p the applied transmembrane pressure, μ the viscosity of the permeate, R_t the total resistance, R_{bm} the resistance of the membrane per se plus the clogging of the membrane pores, R_c the resistance of the filter cake, and R_{cp} the resistance of the concentration polarization layer. Significance of each resistance in membrane filtration is as follows.

The membrane, even in the absence of any suspended particle, has a natural flow resistance. During membrane filtration, particles become attached to the pore channel of the membrane thereby reducing the flow channel dimension, or pores become blocked off completely. The last two effects lead to resistances that are due to adsorption and pore blocking. The blocking filtration model introduced by Hermans and Bredée [1], and Grace [2] is most commonly used as an interpretation of such phenomena.

The clogging of the membrane pores is strongly influenced by such solution environment as pH and the ionic strength. The permeate flux of bovine serum albumin (BSA) (pI 5.1, molecular weight 67,000, Stokes–Einstein diameter 3.55 nm) solution by permeable MF membrane (nominal pore size 0.05 μm) is lowest at around the isoelectric point [3]. As the BSA molecule carries no net charge at the isoelectric point, the molecule is in its most compact state at that point. The BSA molecules deposit themselves rather densely onto the pore walls of the membrane to form a compact configuration with a smaller lateral electrical interaction between the molecules. As a result of this, the flow resistance increases markedly at around the isoelectric point.

In dead-end membrane filtration, which has a feed and permeate stream, each with the same mass flow rate, the resistance of the filter cake plays a major part in the filtration resistance. Therefore, the cake filtration theory can be applied, and thus the permeate flux u_1 is described by

$$u_1 = \frac{p(1 - ms)}{\mu\alpha_{av}\rho s(v + v_m)} \qquad (7.4.2)$$

where m is the ratio of wet to dry cake masses, s the mass fraction of solids in the solution, α_{av} the average specific filtration resistance, ρ the density of

the permeate, and v_m the fictitious filtrate volume per unit membrane area, equivalent to the flow resistance of the membrane [4].

For fine particle suspensions, colloidal forces which arise from interaction between the suspended particles control the nature of the filter cake. The average specific filtration resistance α_{av} and the average porosity ε_{av} of the filter cake are strongly affected by the solution properties, including pH and electrolyte strength. For instance, in MF of suspensions of the titanium dioxide (pI 8.1, the original mean specific surface area size 470 nm), α_{av} goes through a minimum, and ε_{av} is much larger near the isoelectric point [5], as shown in Fig. 7.4.7. The titanium dioxide particles are destabilized around the isoelectric point where the van der Waals attraction is more dominant. Consequently, the particle tends to come together, that is, to flocculate, and the very porous flocs are then formed. Thus, it is speculated that the filter cake formed from such porous flocs has often loose and wet structures. On the other hand, the filter cake becomes compact and dry when the particle carries the charge. Since the most loose filter cake forms around the isoelectric pH, the filter cake is most permeable.

It is interesting to note that the results in protein UF had a distinctly different behavior. In protein UF of BSA solution, the filter cake is in its most compact state around the isoelectric point [6], as shown in Fig. 7.4.8. Since the BSA molecules are hydrophilic colloids, their stability in the solution would appear to be influenced not only by the presence of a surface charge on the protein but also by hydration of the surface layers of the protein. The BSA molecules, because of hydrated layers surrounding them, are not destabilized by such consideration as depression of the electrical double layer. Thus, the BSA molecules have water bound to them even around the isoelectric point. The hydrophilic BSA molecules maintain a dispersed state in the solution due to hydration of the surface layers of the protein even around the isoelectric point. When a BSA molecule acquires a charge, the filter cake becomes loose and wet due to electrostatic repulsion between the charged BSA molecules. This contrasts to the compact filter cake around the isoelectric point. The average specific filtration resistance α_{av} has a definite maximum around the isoelectric point since a compact filter cake provides a large hydraulic flow resistance.

Most membrane filtration processes are operated in the cross-flow mode, in which the feed is moved tangentially to the membrane surface so that the filter cake is continuously sheared off. During membrane filtration, particles in the feed are brought to the upstream surface of the membrane by convective transport, and this results in a higher local concentration of the rejected particles at the membrane surface as compared to the bulk solution which is referred to as concentration polarization [7].

The particle concentration in the solution adjacent to the membrane varies from the value at the membrane surface, C_m, to that in the bulk feed solution, C_b, over a distance equal to the concentration boundary layer thickness δ. The resulting concentration gradient causes the particles to be transported back into the bulk solution due to diffusional effects. At steady state, the rate of convective transport of particle toward the membrane is balanced by the rate of particle transport through the membrane plus the rate of

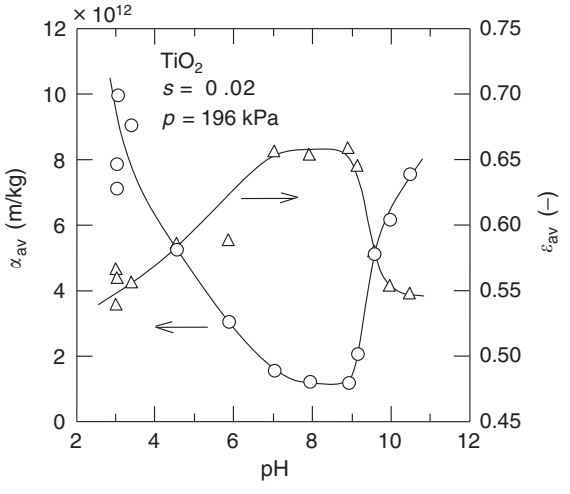

Figure 7.4.7
Effect of pH on average specific filtration resistance and average porosity of filter cake formed in microfiltration of titanium dioxide suspensions.

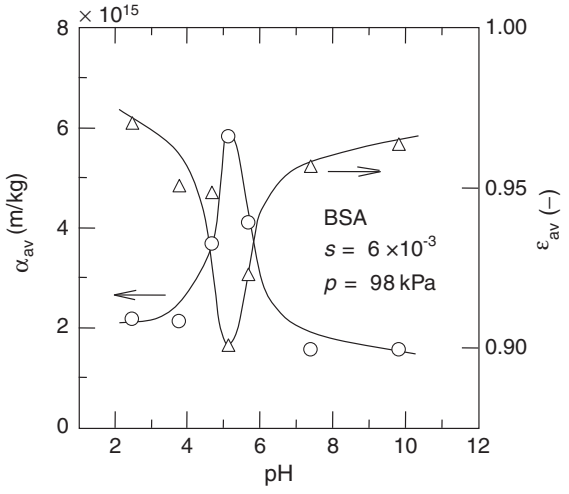

Figure 7.4.8
Effect of pH on average specific filtration resistance and average porosity of filter cake formed in ultrafiltration of BSA solutions.

the diffusive back transport of particle. Thus, the permeate flux u_1 is given by

$$u_1 = k \ln\left(\frac{C_m - C_p}{C_b - C_p}\right) \tag{7.4.3}$$

where C_p is the particle concentration in the permeate, k ($=D/\delta$) the mass transfer coefficient, and D the diffusion coefficient.

The osmotic pressure model assumes that the deviation from pure water flux occurs solely due to the osmotic pressure difference across the membrane, and thus the permeate flux u_1 is given by

$$u_1 = \frac{p - \{\pi(C_m) - \pi(C_p)\}}{\mu R_m} \tag{7.4.4}$$

where π is the osmotic pressure, which is a function of the concentration. Equation (7.4.4) means that the effective driving force across the clean membrane is $p-\{\pi(C_m)-\pi(C_p)\}$. Replacing $p-\{\pi(C_m)-\pi(C_p)\}$ by the hydraulic pressure at the membrane surface, p_m, equation (7.4.4) reduces to the cake filtration equation.

7.4.3.2 Techniques for controlling membrane fouling

To minimize the effects of cake buildup and concentration polarization, membrane filtration is usually conducted using the cross-flow geometry in which the feed flow is parallel to the membrane and perpendicular to the filtrate flow [8]. However, especially in MF the energy requirements associated with pumping the feed (plus any recirculation flow) along the membrane surface are typically very high. Thus, there have been some innovations in recent years with cakeless filtration.

The rotating disk module in which the membrane disk is stationary is suited for large-scale operation [9]. It is possible to enhance the permeate flux by using the vibrating modules [10, 11]. In the rotating cylinder device with the membrane on the inner rotating cylinder, counter-rotating Taylor vortices within the annular gap are available [12, 13]. Dean vortices that twist and spiral in the direction of flow inside a highly curved channel, similar to vortices in rotary modules can result in enhanced flux [14]. These vortices, or flow instabilities, induce turbulence into the system.

Periodic removal of the formed filter cake is also effective for enhancing the permeate flux. Recently, several methods have been investigated: back washing using the filtrate or air pressurization [15], periodic rotation of the cylindrical membrane [16], pulsatile flow [17], high-frequency transmembrane pressure pulsing with a frequency around 0.1–1 Hz [18].

Dead-end upward filtration, where the filtrate flow is in the opposite direction to gravity, and dead-end inclined filtration, where the membrane is inclined, can reduce the cake formation onto the membrane in UF of nanoparticulate suspension and protein solutions. In upward UF of silica sol (mean diameter 6.2 nm) and BSA solution, a sustained permeate flux is achieved, as shown in Fig. 7.4.9 [19, 20], because the filter cake overlying the membrane is exfoliated continuously under the gravitational force acting on the particles comprising the filter cake.

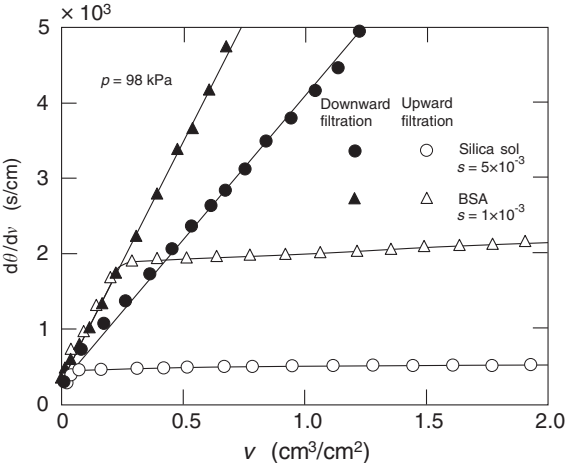

Figure 7.4.9
Permeate flux in dead-end upward ultrafiltration of silica sol and BSA solution.

7.4.3.3 Hybrid operation with membrane filtration

Another approach for enhancing the permeate flux is to employ external force fields. Electrofiltration, in which an applied electric field is used to drive charged particles away from the membrane surface, has been developed. In electrofiltration, the accumulation of the particles on the membrane surface is limited by the imposed electrophoretic force. In addition, the permeate flux through the filter cake is dramatically enhanced due to electroosmosis as a secondary electrokinetic phenomenon. This method can be applied to a broad combination ranging from MF of particulate suspension such as bentonite [21] to UF of protein solution. Fig. 7.4.10 shows the reciprocal permeate flux ($d\theta/dv$) versus the permeate volume per unit membrane area, v, for various values of the strength of the DC electric field, E [22]. The steady permeate flux increases noticeably with the magnitude of the imposed field strength. Also, a higher electric field strength causes the permeate flux to equilibrate more rapidly.

A method has been developed for removing humic substances by hybrid UF combined with both

flocculation and adsorption treatments, as shown in Fig. 7.4.11 [23]. Flocculation by use of polyaluminum chloride (PACl) is particularly effective for the removal of humic acids, which constitute the relatively high molecular weight fractions of humic substances, whereas adsorption by use of powdered activated carbon (PAC) is able to remove fulvic acids of relatively low molecular weight effectively, which cannot be fully flocculated by PACl. Hybrid UF in combination with flocculation and adsorption

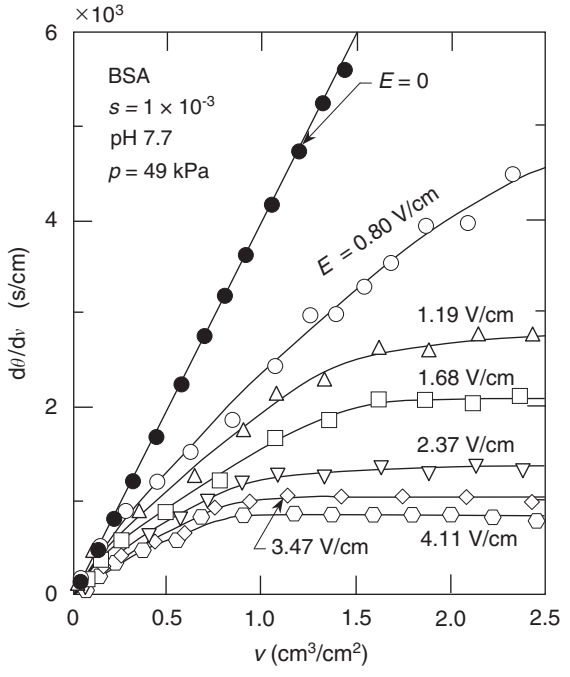

Figure 7.4.10
Permeate flux in electro-ultrafiltration of BSA solution.

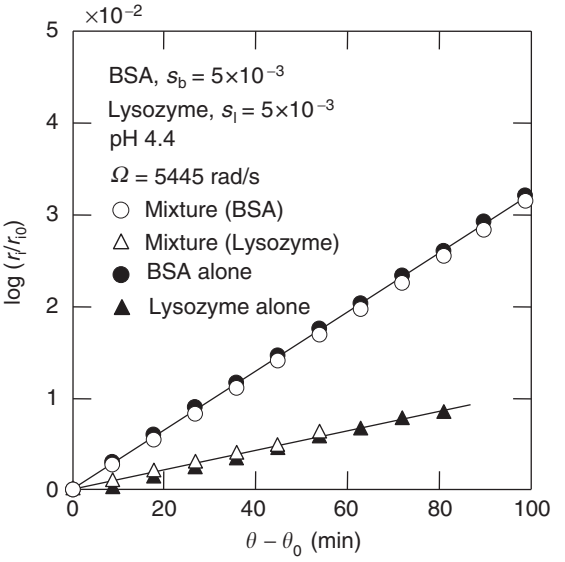

Figure 7.4.12
Behaviors of ultracentrifugal sedimentation of binary protein mixtures at pH 4.4.

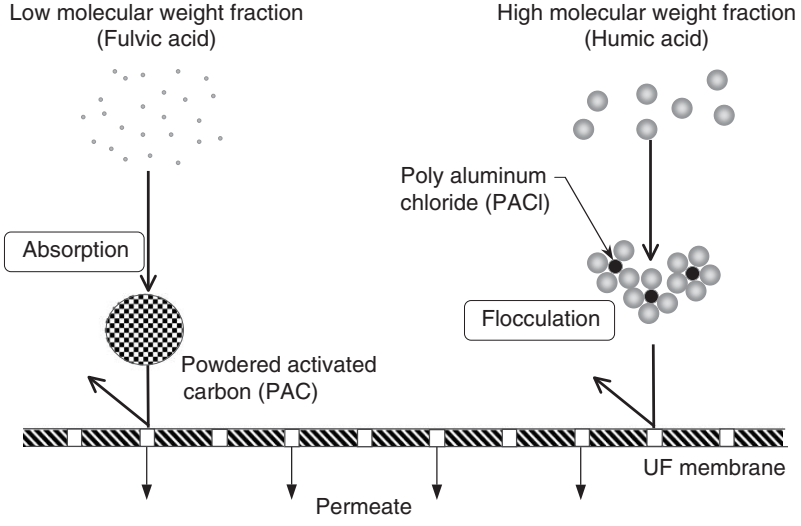

Figure 7.4.11
Mechanism of hybrid ultrafiltration of humic substances combined with both flocculation and adsorption treatments.

treatments exhibits high permeate quality because the flocs and PAC are easily retained by the UF membrane.

7.4.3.4 Ultracentrifugal sedimentation

In ultracentrifugal sedimentation, ultracentrifugal force field of several tens of thousands of revolutions per minute is applied to a rotor. In recent years, ultracentrifugal sedimentation is employed for concentrating dilute protein solutions and for separating proteins and other large biological molecules from low-molecular-weight solutes or from much larger particles. Fig. 7.4.12 shows the results for ultracentrifugal sedimentation of an aqueous solution of the mixtures of BSA and egg white lysozyme (pI 11.0, MW 14,300) measured using Schlieren optics in an analytical ultracentrifuge [24]. The angular acceleration Ω of the rotor is 5,445 rad/s. The symbol r_i and r_{i0} in the figure represent the distances from the center of rotation to the sedimentation boundary at time θ and θ_0, respectively. The electrical nature of macromolecules plays a significant role in determining the sedimentation behavior in ultracentrifugation of binary protein mixtures. In the pH range where both protein molecules were electropositive, the molecules sediment independently due to the electrostatic repulsive force acting between BSA and lysozyme molecules.

References

[1] P.H. Hermans, H.L. Bredée: *J. Soc. Chem. Ind.*, **55T**, 1–4 (1936).

[2] H.P. Grace: *AIChE J.*, **2**, 307–336 (1956).

[3] E. Iritani, Y. Mukai, Y. Tanaka and T. Murase: *J. Membr. Sci.*, **103**, 181–191 (1995).

[4] B.F. Ruth, G.H. Montillon and R.E. Montanna: *Ind. Eng. Chem.*, **25**, 153–161 (1933).

[5] E. Iritani, Y. Toyoda and T. Murase: *J. Chem. Eng. Jpn.*, **30**, 614–619 (1997).

[6] E. Iritani, S. Nakatsuka, S. Aoki and T. Murase: *J. Chem. Eng. Jpn.*, **24**, 177–183 (1991).

[7] S. Kimura, S. Sourirajan: *AIChE J.*, **13**, 497–503 (1967).

[8] J. Murkes, C.G. Carlsson: Crossflow filtration: Theory and practice, Wiley, NY (1988).

[9] T. Toda: in *Encyclopedia of Fluid Mechanics: Slurry Flow Technology*, N.P. Cheremisinoff (Ed.), Gulf Publishing, Houston, TX, p. 1149 (1985).

[10] B. Culkin, A.D. Armando: *Filtr. Sep.*, **29**, 376–378 (1992).

[11] T. Murase, E. Iritani, P. Chidpong, K. Yagishita, K. Yoshida, T. Sugiyama and M. Shirato: *Kagaku Kogaku Ronbunshu*, **14**, 135–140 (1988).

[12] W. Tobler: *Filtr. Sep.*, **19**, 329–332 (1982).

[13] T. Murase, E. Iritani, P. Chidpong, K. Kano, K. Atsumi and M. Shirato: *Kagaku Kogaku Ronbunshu*, **15**, 630–637 (1989).

[14] K.-Y. Chung, R. Bates and G. Belfort: *J. Membr. Sci.*, **81**, 139–150 (1993).

[15] V. Gekas, B. Hallström: *Desalination*, **77**, 195–218 (1990).

[16] T. Murase, E. Iritani, P. Chidpong and K. Kano: *Kagaku Kogaku Ronbunshu*, **15**, 1179–1186 (1989).

[17] V.G.J. Rodgers, R.E. Sparks: *J. Membr. Sci.*, **68**, 149–168 (1992).

[18] S.M. Finnigan, J.A. Howell: *Trans. IChemE*, *Part A* (*Chem. Eng. Res. Des.*), **70**, 527–536 (1992).

[19] E. Iritani, T. Watanabe and T. Murase: *Kagaku Kogaku Ronbunshu*, **17**, 206–209 (1991).

[20] E. Iritani, T. Watanabe and T. Murase: *J. Membr. Sci.*, **69**, 87–97 (1992).

[21] H. Yukawa, K. Kobayashi, Y. Tsukui, S. Yamano and M. Iwata: *J. Chem. Eng. Jpn.*, **9**, 396–401 (1976).

[22] E. Iritani, K. Ohashi and T. Murase: *J. Chem. Eng. Jpn.*, **25**, 383–388 (1992).

[23] E. Iritani, Y. Mukai, N. Katagiri and T. Hirano: *Kagaku Kogaku Ronbunshu*, **30**, 353–359 (2004).

[24] E. Iritani, S. Akatsuka and T. Murase: *Kagaku Kogaku Ronbunshu*, **23**, 224–229 (1997).